



**Università
degli Studi
di Ferrara**



UCA

Universidad
de Cádiz

International Ph.D. Course
in
Earth and Marine Sciences

CYCLE XXXI

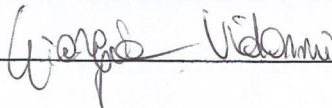
DIRECTOR Prof. Massimo Coltorti

**DAMAGE PROCESSES ON STONES IN URBAN ENVIRONMENT:
FIELD EXPOSURE TESTS AND LABORATORY ANALYSES
CONTRIBUTING TO POLLUTION IMPACT EVALUATION**

Scientific/Disciplinary Sector (SDS) GEO/09

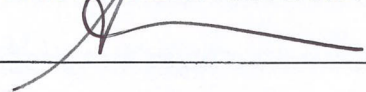
Candidate

Dott. VIDORNI GIORGIA



Supervisors

Prof. BONAZZA ALESSANDRA



Prof. VACCARO CARMELA



Years 2015/2018

INDEX

<u>ABSTRACT</u>	i
<u>INTRODUCTION</u>	1
<u>1. CHAPTER 1 - STATE OF THE ART</u>	3
1.1. POLLUTION IMPACT ON CULTURAL HERITAGE	3
1.1.1. EVOLUTION OF POLLUTION: PAST, PRESENT AND FUTURE	7
1.2. DIFFERENT APPROACHES FOR STUDYING DAMAGES TO HISTORIC STONE SUBSTRATES INDUCED BY AIR POLLUTION	12
1.2.1. SAMPLING FROM HISTORIC BUILDINGS	12
1.2.2. TEST CARRIED OUT IN SIMULATION CHAMBER	21
1.2.3. FIELD EXPOSURE TESTS	24
1.3. DAMAGE FUCTIONS	30
<u>2. CHAPTER 2 - MATHERIALS AND METHODS</u>	36
2.1. FIELD EXPOSURE TESTS	36
2.1.1. SITES DESCRIPTION OF FIELD EXPOSURE TEST	37
2.1.2. ANALYSES PERFORMED	50
2.2. PARTICULATE MATTER MONITORING CAMPAIGNS	57
2.2.1. ANALYSES PERFORMED	61
<u>3. CHAPTER 3 - RESULTS AND DISCUSSIONS</u>	65
3.1. FIELD EXPOSURE TESTS OF STONE SAMPLES	65
3.1.1. MINERALOGICAL-PETROGRAPHIC CHARACTERISATION OF STONE SAMPLES	65
3.1.1.1. <i>Visual assessment and Observation of thin sections by Polarized Light Microscopy (PLM)</i>	65
3.1.1.2. <i>X-Ray Powder Diffraction (XRPD)</i>	71
3.1.1.3. <i>X-Ray Fluorescence Spectroscopy (XRF)</i>	73
3.1.1.4. <i>Mercury Intrusion Porosimetry (MIP)</i>	75
3.1.2. COLORIMETRIC ANALYSIS	79

3.1.3. TOTAL DEPOSITED PARTICULATE (TDP)	105
3.1.4. ION CHROMATOGRAPHY (IC)	109
3.1.5. CARBON SPECIATION AND RELATED ISOTOPIC ANALYSIS	138
3.1.6. ENVIRONMENTAL SCANNING ELECTRON MICROSCOPY (ESEM-EDX)	167
3.1.7. INDUCTIVELY COUPLED PLASMA MASS SPECTROMETRY (ICP-MS)	190
3.2. FIELD EXPOSURE TESTS OF PASSIVE FILTERS	198
3.2.1. TOTAL DEPOSITED PARTICULATE (TDP)	198
3.2.2. ION CHROMATOGRAPHY (IC)	201
3.2.3. CARBON SPECIATION	206
3.3. PARTICULATE MATTER MONITORING CAMPAIGNS	209
3.3.1. CHARACTERISATION OF EXPOSURE SITES	209
3.3.2. TOTAL SUSPENDED PARTICULATE	250
3.3.3. ION CHROMATOGRAPHY (IC)	260
3.3.4. CARBON SPECIATION	273
3.3.5. BIOAEROSOL	284
4. <u>CHAPTER 4 - SIGNIFICANCE OF CHANGES OF EXPOSED MATERIALS</u>	294
5. <u>CHAPTER 5 - FINAL CONSIDERATIONS</u>	307
5.1. CONCLUSIONS	307
5.2. FUTURE PERSPECTIVES	308
<u>ACKNOWLEDGMENTS</u>	309
<u>REFERENCES</u>	310
<u>ANNEX 1 - DIFFRACTION DATA</u>	328
<u>ANNEX 2 – COLORIMETRIC DATA</u>	332
<u>ANNEX 3 – WATER-SOLUBLE DATA OF STONE DEPOSIT</u>	335

<u>ANNEX 4 – CARBON FRACTIONS OF STONE DEPOSIT</u>	338
<u>ANNEX 5 – WATER-SOLUBLE DATA OF PASSIVE FILTERS</u>	341
<u>ANNEX 6 – TOTAL SUSPENDED PARTICULATE</u>	343
<u>ANNEX 7 – WATER-SOLUBLE DATA OF PM MONITORING CAMPAIGNS</u>	347
<u>ANNEX 8 – PUBLICATIONS, PROCEEDINGS, PRESENTATIONS</u>	351

ABSTRACT

Air pollution constantly threatens the conservation of carbonate stone monuments and built heritage mainly in urban areas. Even if different studies focused on the effect of pollution on stone materials, by analysing samples collected from historic buildings, performing tests in simulation chamber and/or in field and monitoring air quality (gases and aerosol) of the environment surrounding specific cultural heritage, lack of knowledge still remains in the quantitative correlation between the concentration of particular atmospheric pollutants and their damage induced to stone. Furthermore, the possible repercussions on built heritage of the current atmosphere in Western Europe, poorer than in the past of SO₂ but richer of NO_x and organic compounds, merit consideration.

In this regard, the Institute of Atmospheric Sciences and Climate of the National Research Council of Italy (ISAC-CNR) with the Department of Physics and Earth Sciences of the University of Ferrara performed field exposure tests of stone model samples and passive filters for 24 months in Italian cities characterised by different environmental conditions (i.e. Bologna, Ferrara and Florence) associated with particulate matter monitoring campaigns as a non-invasive methodological approach for studying the impact of urban pollution on carbonate stones. Marble (Carrara Marble) and limestone (Verona Red Marble) were selected as model samples as they were widely used as construction and ornamental elements in historic Italian architecture and for their physico-chemical features. Galvanized metallic racks were prepared to host samples with different exposure orientations (i.e. horizontal, oblique and vertical) in order to identify how positioning may reflect on deposition and removal of pollutants. Polished stone samples were exposed outdoor, partially sheltered from the rain wash-out, in areas strongly affected by pollution due to vehicular traffic. At defined time intervals, several analytical techniques (Colorimetric analysis, IC, EA-IRMS, ESEM-EDX, ICP-MS) were used for characterising the state of degradation of the exposed stone specimens while aerosol monitoring campaigns allowed to compare the atmospheric components (in terms of soluble and carbon fractions) with those actually accumulate on samples surface and passive filters.

The results demonstrate an increasing trend of soiling over time in all sites, more evident in horizontal and oblique marble samples. In particular, blackening and yellowing processes of stone surface were identified in relation with deposition of elemental carbon (EC) and accumulation of organic carbon (OC) and sulphate, respectively. The adopted methodological approach provided information about the real deposition of soluble and carbon fractions per surface unit over time as well as the development of methodology for carbon speciation by thermally-based separation allowed to measure C fractions in damage layers without any chemical attack. Moreover, the high concentration of heavy metals on stone deposit, the prevalence of OC over EC both in atmosphere and in deposit of stone samples and passive filters as well as soluble ions (mainly Cl⁻ and SO₄²⁻ in deposit and NO₃⁻, SO₄²⁻ and NH₄⁺ in atmospheric PM) confirm as vehicular traffic has directly (combustion of fossil fuels) or indirectly (re-suspended dust and de-icing salts) affected the composition of the deposited particulate matter.

INTRODUCTION

Air pollution still remains an outstanding problem not only for human health and preservation of the environment but also for the conservation of cultural heritage. In particular, monuments and built heritage located in urban sites are particularly affected by this issue as many concurrent emission sources (mainly vehicular traffic and heating systems) gather in a relative small area. Beside an irreversible loss of value of works of art, the decay of cultural heritage implies expansive conservation and restoration works. For these reasons, the study of factors and mechanisms involved in the decay of historic monuments and buildings is of primary importance to plan preventive strategies of protection and safeguarding.

In this regard, studies of pollution impact over the past few decades were mostly related to marble and limestone, widely employed everywhere as constructional and decorative materials, characterised by low porosity and chemical homogeneity (mainly composed by calcium carbonate). It is widely known that SO₂ reacts with carbonate stones to cause the formation of gypsum through sulphation process and that particulate matter, and in particular its carbonaceous fractions, has a driving role in soiling and black crusts formation. The black component of carbonaceous aerosol, also known as elemental carbon (EC) or soot and produced by incomplete combustion processes, is responsible for the dark colour of damage layer. Nevertheless, sulphation process, which became the dominant responsible of air pollution impact on stone at the end of the nineteenth century, has underwent a decrease because mitigations policies as well as use of low-S fuels have reduced the emissions of SO₂ in atmosphere from the mid-20th century. Beside the ongoing drop of SO₂, higher concentration of NO_x and organic compounds deriving from vehicular traffic is detected in the majority of Western Europe cities. The shift in atmospheric composition from SO₂ dominated to multipollutant dominated situation is also reflected in a color change of the damage layers from dark to greyish and brownish tones and it is expected to increase over time. Moreover, NO_x can interact with the stone substrate in the form of very soluble salts, generating microcracks due to significant changes of salts volume.

Literature highlights that impact of air pollution on stone monuments has been mostly assessed by comprehensive analyses on specimens collected from historic built heritage to investigate the results of air pollution-stone interaction and by test in simulation chamber to better understand the role of different parameters with potential impact in deterioration phenomena and the related processes of damage in a simplified system. Additionally, field exposure tests are gaining more relevance as they allow to study the ongoing environmental interactions on different materials in the same or different climate conditions. In this context, atmospheric monitoring campaigns performed outdoor close to historic monuments provide further information about those gases and particles potentially dangerous for the conservation of the cultural heritage but they are still scarce.

The combination of field exposure tests of stone materials and passive filters with simultaneous aerosol monitoring campaigns may have high potential for identifying the main emission sources in atmosphere in a specific site and gradually monitoring the related variations that happen on the exposed materials. This approach would contribute to develop damage and dose-response functions useful to quantify the effect of pollution on cultural heritage and thus plan long-term strategies for built heritage management. In this regard, the Institute of Atmospheric Sciences and Climate of the National Research Council of Italy (ISAC-CNR, Bologna) and the Department of Physics and Earth Sciences of the University of Ferrara are collaborating to study the impact of urban atmospheric pollution on carbonate stones by performing field exposure tests for 24 months in Italian cities characterised by different environmental conditions (i.e. Bologna, Ferrara and Florence). The selected lithotypes are a marble (Carrara Marble – CM) and a limestone (Rosso Ammonitico Veronese hereafter called with the commercial name Verona Red Marble – VRM). The doctorate research intends to monitor over time and quantify (in terms of soluble and carbon fractions) the material accumulated on the exposed surface of stone samples in order find a possible interaction with colorimetric and chemical changes of stones. In particular, chemical components of deposited material was

analysed for assessing the mass of soluble and carbon fractions per surface unit on stone specimens and passive filters. Further information would be collected by weekly monitoring campaigns of particulate matter performed every 6 months close to the selected sites for correlating the soluble and carbon fractions present into atmosphere with those fractions detected on stone surface and potentially dangerous for its conservation.

In order to have a complete comprehension of pollution impact on cultural heritage, an overview of the state of the art will be presented in Chapter 1, focusing on the main atmospheric components that cause deterioration to stone substrate, their variation over time, approaches utilised for studying their impact on built materials as well as possible damage functions suitable for planning preventive conservation interventions.

Afterwards, the thesis will focus on the description of field exposure tests, with particular regard to the selected exposure sites and adopted methodology for assessing colour variation of stone samples and characterising the composition of deposited particulate on stone and passive filters as well as on illustration of particulate matter monitoring campaigns (Chapter 2).

After a mineralo-petrographic description of stone samples and identification of their physical (porosity) and elemental features, Chapter 3 will display and examine outcomes of colour changes of stone specimens and of characterisation of deposited particulate matter, in terms of chemical composition (soluble ions, carbon fractions and elemental components) and morphology. These results will be compared with those obtained from passive filters exposed in the same environmental conditions (Chapter 3, 4). In addition to an environmental description of each selected site, Chapter 3 will present and discuss also data obtained from monitoring campaigns of atmospheric particulate matter and bioaerosol in order to relate soluble and carbon fractions measured in atmosphere with those identified in the deposit.

In conclusion, this research work contributed to create a database concerning the real deposition of particulate matter (in terms of soluble and carbon fractions) on stone surface respect to that monitored in atmosphere and the consequent variation of the colorimetric parameters. These data will be useful to improve damage functions suitable for conservation interventions and identify threshold level of air quality proper for the conservation of cultural heritage (Chapter 5).

1. CHAPTER 1 - STATE OF THE ART

1.1. POLLUTION IMPACT ON CULTURAL HERITAGE

Stones have been widely used as construction materials for historic monuments and buildings. Their exposure outdoors for long time has therefore led them to cope with the interaction and changes of the surrounding environment. Since most of the historic buildings are located in city, pollution of urban areas (mainly induced by industry, transport and energy production) adds a supplementary cause of damage to their weathering occurring in a natural environment due to the process of time. Indeed, even if climate change impact is an increasing problem that threatens the conservation of worldwide cultural heritage and is attracting the attention of the European Commission (for example the FP6 – “pioneer project” NOAH’s ARK_Sabbioni et al., 2007; the FP7 CLIMATE FOR CULTURE_Kramer et al., 2013 and Sabbioni et al., 2012), stone decay induced by atmospheric pollution still remain an outstanding issue in urban environment, with remarkable cultural and economic consequences. The perpetuation of the decay of built heritage induces in fact to an irreversible loss of such an invaluable and irreplaceable good as well as requires expensive restoration and conservation activities. Therefore, it is necessary to fully investigate the main causes of damage of cultural heritage in order to plan specific action of safeguard.

The mechanisms by which air pollution induces damages to stone are numerous such as soiling of light-coloured stone surfaces, crystallization of soluble and insoluble salts inside the porous network (with related problem of surface decohesion and exfoliation) and corrosion induced by acid pollutants that decrease the natural pH of rains and fog (Amoroso, 2002; Watt et al., 2009). These different degradation phenomena are strictly influenced by the intrinsic features of the building materials, their location and exposure to the pollutant sources. Hereafter a brief examination of these main damage typologies will be displayed.

Soiling is a visual nuisance resulting from the temporary settling of particulate matter (PM) on building materials surface causing, at sufficiently high concentrations, a change in colour and/or reflectance. On stone surface, external ions and atoms are not completely balanced and therefore tend to easily attract particles suspended in the air. Anyway, particles deposition happens on non-reactive surface, it means there is no chemical change of stone substrate, and therefore this accumulation can be removed by washing (Watt et al., 2009). Many and complex factors influence the settling, accumulation and removal process of particles, depending on the chemical composition, concentration and size of particles as well as the inherent characteristics of substrate materials and its interaction with the surrounding environment.

The major contribution to the process of soiling is the deposition of particulate matter and therefore of a complex mixture of substances coming from various sources. Airborne particulate matter could be emitted directly into the atmosphere from a source (*primary particulate material*) or could results from the reaction of two gases or vapours that condense onto a nucleus (*secondary particulate matter*). Emissions from vehicular fossil fuel burning, chimney stacks and those derived from the re-suspension of soil and dust by wind/ traffic/ mechanical disturbance (such as quarrying) are examples of primary particulate matter while the oxidation of sulphur dioxide droplets or nitrogen oxide vapour to sulphuric acid or nitric acid, respectively, belong to secondary PM. Each source emits particles with characteristic size and chemical composition, influencing the soiling process (Watt and Hamilton, 2003). Anthropogenic sources, such as vehicular traffic and industry emissions, are responsible for the major release of fine PM (i.e. particles with a diameter < 1 µm), which is mainly composed by carbonaceous particles and minor inorganic salts. On the contrary, the concentration of insoluble minerals is predominant in coarser particulate matter ($\phi > 1 \mu\text{m}$) and derived mostly from natural sources such as erosion, soil dust re-suspension, sea spray as well as pollens, mould spores and bacterial cells. The higher concentration of carbonaceous compounds in city leads to the

soiling of building materials to be enhanced in urban environment in respect to rural one (Grossi et al., 2003). In particular, these particles are present in PM in three forms:

1. *Carbonate carbon (CC)*: it derives essentially from construction materials, soil-derived minerals and re-suspension of dust. CC represents a small amount of the total mass of particulate, mainly in the coarse mode;
2. *Elemental carbon (EC)*: it is the responsible for the dark colour of soiling and is therefore also known as “black carbon”, due to its high retention on surfaces and high optical absorptivity. It mainly derives from incomplete combustion of fossil fuels used for transportation, heating and power generation; in particular, Hamilton and Mansfield (1991) identified diesel emissions as the main source of particulate elemental carbon (PEC). Moreover, PEC acts as catalytic site for atmospheric reactions and as a carrier for condensed vapours (Watt and Hamilton, 2003);
3. *Organic carbon (OC)*: it represents the 60-80% of the atmospheric carbonaceous particulate matter. Biological weathering, decayed protective organic treatments, primary condensates (alkanes – C17-C36–, alkenes, aromatics and polyaromatics originated directly from incomplete combustion of fossil fuels and absorbed onto the PM surface) and oxidised hydrocarbons are identified as the different sources of OC (Bonazza et al., 2005). Moreover, OC could be also of secondary origin due to the condensation of compounds in the atmosphere by photo-oxidation of volatile organic precursors (Gordon et al., 2012). Watt and Hamilton (2003) reported that OC increases also the adhesiveness of the particulate matter once deposited on the built substrate, enhancing the accumulation of particles on the building surface.

Brimblecombe and Grossi (2004) ascribed the blackening of soiling mainly to particulate elemental carbon but also coal dust, in the coarse mode, can contribute to soiling. The latter have a short residence time in the atmosphere and therefore, when detected, it is ascribable to local sources.

Besides the chemical composition and concentration of particles, the rate of soiling is highly influenced also by surface roughness and kind of porosity of the stone on which particles impinge. Substrate with a rough surface is able to easily catch and stick PM, preventing its removal by the action of rain or wind. Grossi et al. (2003) proved also that a rough surface undergoes a higher soiling effect than a porous stone characterised by large open pores on surface. Moreover, it is really important to consider also how the stone substrate is exposed to rainfall. Even if moisture on building surface enhances dry deposition of air pollutants, sheltered stones are affected by higher soiling effect. On the contrary, as rainwater runs across the unsheltered surfaces, the previously deposited particles and the altered substrate materials can be removed or redistributed. Indeed, rainwater containing dissolved carbon dioxide, responsible for decreasing rain pH (about 5,6 or even lower in the presence of sulphate and nitrate), is able to solubilise carbonate stones and hence create calcium bicarbonate, $\text{Ca}(\text{HCO}_3)_2$. This could be partly leached out by rain (*surface recession* or *leaching*) or it could re-precipitate as calcium carbonate by the evaporation of water. The newly formed CaCO_3 is a powder, with higher exposure surface and therefore more prone to acid attacks than the original crystals (Amoroso, 2002). In addition to chemical dissolution, rainwater carries out also a mechanical action on stone substrate, abrading it with solid particles picked up during its flow. Furthermore, the amount of rain striking a surface is highly dependent also on the unobstructed wind speed and wind direction, that allow reaching building areas usually sheltered from rainwater (Tang et al., 2004; Tang and Davidson, 2004). Finally, the geometry of surfaces and the climatic characteristic of the environment considerably affect the soiling pattern of building materials, since they are related to the deposition phenomena of particulate matter. Sheltered horizontal surfaces soil faster than vertical ones because of the *gravitational settling* of coarse particles that, even if they are present in minor concentration than fine particles in a mass area, are able to cover a bigger surface area (Watt et al., 2009). In addition to the permanent *Brownian diffusion* (induced by

the collision with fast-moving air molecules) of ultrafine particles ($\phi < 0,1 \mu\text{m}$) and gravitational settling of coarse particles, particulate matter could be deposited through:

- *Thermophoresis*: in presence heat gradient, fine particles tend to follow the air flow that aspires to reach a situation of more stability (from higher temperature to lower one);
- *Stefan flow* due to the flow of water vapour during condensation (with deposition of particles on surface) or evaporation (and removal of PM) phenomena;
- *Inertial impaction*: following the air mass in presence of a turbulence, fine particles avoid the coming obstacle (such as a wall) while the too heavy coarse particles impinge on it.

As the deposited pollutants chemically react with the substrate, there is the crystallization of a compact surface layer with a chemical composition different from the original material. Gypsum crusts are the most common kind of growth found on historic buildings surface (Figure 1.1).

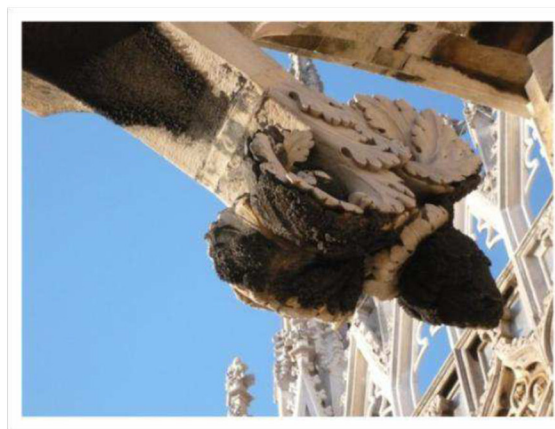
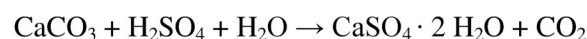


Figure 1.1 Gypsum crust on decoration of buttress at Milan Cathedral.

Calcareous stones are vulnerable towards dry and wet deposition of atmospheric sulphur dioxide, SO_2 . In presence of water, this reacts with the calcium carbonate of the substrate, CaCO_3 , leading to the formation of gypsum, $\text{CaSO}_4 \cdot 2\text{H}_2\text{O}$, through the widely studied sulphation process:



In dry sulphation process, SO_2 is deposited on stone surface and, in presence of moisture, reacts with the CaCO_3 to form calcium sulphite as intermediate product, which then undergoes further oxidation to gypsum. Additionally, SO_2 could be transformed directly in atmosphere or on stone to sulphuric acid that reacts with CaCO_3 to produce $\text{CaSO}_4 \cdot 2\text{H}_2\text{O}$. In general, sulphation process is enhanced by the presence of ozone, O_3 , mainly at high relative humidity: O_3 , acting as oxidiser, increase the rate of conversion of sulphites and sulphates (Sabbioni, 2003).

The formation of gypsum crystals in place of calcium carbonate minerals in the stone is not only a product of decay but it could represent a cause of weathering itself (Amoroso, 2002). In effect, gypsum has a much higher molecular volume than the carbonate mineral, which may cause mechanical stresses in pores and cracks of the substrate. Furthermore, the linear coefficient of thermal expansion of gypsum is about five times that of calcite, which is further enhanced when black particles, embedded in the crust, induce a higher absorption of solar radiation than white surfaces. Gypsum is also more soluble than the carbonates, so in presence of rain it can be removed easily via dissolution, laying bare the original rock. Nevertheless, in not

rain washed areas, the development of gypsum crust will reduce the permeability of the carbonate substrate and in turn intensify the water retention beneath.

The chemical composition as well as the porosity of the stone substrate is an influential parameter in the sulphation process of architectural heritage. Stones mainly composed of calcium carbonate (or more rarely of calcium magnesium carbonate) and characterised by low porosity, such as marble and limestone, display three different typologies of damage depending how rainwater wets the monument surfaces (Sabbioni, 2003):

1. *Black areas*. This pattern is representative of stone surfaces exposed outdoors but partially sheltered from intense runoff and washout of rains. Therefore, atmospheric gases and particles could deposit and interact with the substrate by the presence of adequate water contents. In particular, surfaces of monuments and buildings built with limestone and marble are often covered by compact black crusts of gypsum. The blackening of the crusts is induced by the presence of carbonaceous particles coming from combustion processes and trapped into gypsum. Besides the chromatic variation, carbonaceous particles, emitted by oil fuelled power plants and domestic heating systems, seems to accelerate the SO₂ oxidation process on stone surface because of their heavy metal content (Sabbioni, 2003). In particular, soot and metallic particles (mainly Fe, Cr, Ni, Cu and Mn) emitted by diesel engines play the most significant role in the oxidation of SO₂; emissions from gasoline engine exhaust, composed mostly by Pb and Br and to less extent by soot, cause in less gypsum formation.
2. *Grey areas*. These typologies are found on sheltered surfaces, where atmospheric pollutants accumulate by dry deposition only and the humidity (from fog and dew) is not enough to create products of reactions between stone substrate and atmospheric gas and aerosol.
3. *White areas*. The surfaces exposed directly to rainwater and, therefore, subjected to water runoff undergo to dissolution of the carbonate rock, leading to resurface the original stone colour. This is also emphasised by the repeatedly removal of particulate matter deposited on surfaces. Furthermore, some authors (Török, 2003; Török and Rozgonyi, 2004) distinguished the presence of two white crusts on oolitic limestone, widely utilised in the Budapest architecture: thin crusts and thick, hard crusts. Both are characterised by the re-precipitation of calcite on outer, exposed surfaces while gypsum accumulated on the underside of the crusts. With crystal growth, gypsum exerts high pressure on pore walls and thus blisters the thin, fragile white crusts. Meanwhile, in the thick crusts, gypsum fills the pores, making the crust impermeable. In this case, as long as weathering factors (such as salt crystallisation, freeze-thaw cycles and thermal expansion) do not threaten the integrity of the compact crust, it behaves as an impermeable case-hardened layer on the stone surface.

In the case of high porous stones, such as sandstone and calcarenite, a homogeneous blackening covers the whole surface independently of its geometry and exposure to rain (Sabbioni, 2003). The intrinsic features of these stones are the responsible for the development of this uniform blackened damage layer. In effect, the high degree of roughness, due to the porosity of sandstone and calcarenite and their mineralogical inhomogeneity, increases the deposition of particles present into the atmosphere respect to smooth and low porous surfaces and inhibits their removal and leaching by rainwater (Sabbioni and Zappia, 1992a). Moreover, their pores and capillaries hold humidity back, encouraging the reaction of atmospheric particles and gases with the stone substrate. In particular, two damage layers are observable on sandstone and calcarenite (Sabbioni, 2003):

1. *A thin surface layer (A)* with a thickness of few millimetres and mainly composed by gypsum and embedding carbonaceous particles (a composition similar to the black crusts collected from

marbles and limestones). This layer derives from the sulphation process that converts calcium carbonate presents in the cement or even as grains in calcarenite into gypsum. Moreover, the presence of carbonaceous particles entails the dark colour to the damage layer. As a consequence, stone albedo is decreased, enhancing the absorption of solar radiation and promoting higher thermal expansion, heating/cooling cycles and wetting/drying cycles.

2. *An underlying, thicker (cm), disaggregated layer (B)* subjected mainly to dissolution, caused by acid precipitations and accountable of the decohesion of sandy grains, and secondly to partial sulphation process.

The instability of layer B and the stress caused by gypsum hydration/dehydration cycles in the outermost layer induce also to the detachment of the upper layer A, laying bare the original rock. Thus the unaltered stone is exposed to outdoors and a new cycle of weathering starts again.

Less attention has been paid to the study of the pollution impact on granites even if they are widely present in cultural heritage and reveal good resistance to weathering because of their low porosity and chemical composition (Bonazza and Sabbioni, 2016). However, some studies (Schiavon, 2007; Graue et al., 2013) have highlighted as anthropogenic SO₂ is responsible for the deterioration of igneous rock as well as for the afore-mentioned stones. Specifically, Schiavon (2007) identified the dual role of this pollutant in granite: the sulphation of calcium bearing minerals (such as anorthite) leading to the formation of gypsum crystals and the acceleration of kaolinisation of feldspars in urban environment. Nevertheless, the concentration of calcium in granite is not sufficient to explain the large quantities of gypsum often observed in granitic historic buildings. Some studies (Silva Hermo et al., 2010) ascribed the principal origin of gypsum to plasterworks and paintings that in ancient times decorated the stone substrate or to joint mortars.

Even though urban air pollution induces damages to different typologies of stone, as described above, carbonate stones with low porosity undergo a more severe damage and its relative chemical homogeneity and low porosity have permitted the unification of weathering mechanisms within few simple models and facilitated the comprehension of the damage phenomena. Additionally, limestone and marble were broadly employed as construction and decorative materials by different civilisations and in different historical periods, and therefore require to be best preserved.

1.1.1. EVOLUTION OF POLLUTION: PAST, PRESENT AND FUTURE

Urban air pollution is an issue that has called special attention to society mainly in the last centuries but it has threatened the safeguard of historic buildings and monuments in varying degrees since ancient time. The atmospheric composition of cities has in effect been altered during time by the introduction and replacement of various anthropogenic pollution sources, influencing the nuance and appearance of stone materials. It is worth to consider that the decay induced to built heritage is related to the impact of the overall surrounding environment over the entire lifetime of the building and thus the damaging process is likely cumulative. Therefore, the study of air pollution history proves to be really important in understanding the proper protection activities to be carried out on the building.

The effects of urban air pollution were known since classical times and primarily directed towards human health. Seneca, writing to Lucilio (Epistulae morales ad Lucilium 104, 6), complained about the stink, soot and heavy air of Rome that forced him to find refuge in his small farm in Numentum for health reasons:

“Ut primum gravitatem urbis excessi et illum odorem culinarum fumantium quae motae quidquid pestiferi vaporis sorbuerunt cum pulvere effundunt, protinus mutatam valetudinem sensi.”

Nevertheless, some evidences of the damaging outcome of pollution on buildings were also present in ancient literature. For example, poet Horace criticised smoke blackening to temples in Rome induced by the enormous amount of wood consumed by population (Brimblecombe and Camuffo, 2003). Moreover, even paintings can provide useful information about the appearance of cultural heritage and the related effects of pollution in the past. In this regard, Professor Dario Camuffo, working within the ENV4-CT95-0092 EC Project “Archeometric study to reconstruct the pollution and the climate of the past and their effects on cultural property (ARCHEO)”, has highlighted how the vedutisti painters were able to reproduce high-detailed and realistic cityscapes, as in the case of “Grand Canal: Looking South-West from the Palazzo Grimani to the Palazzo Foscari” (1735) painted by Giovanni Antonio Canal, better known as Canaletto. Focusing on Palazzo Grimani is possible to notice the blackening of the lower part of façade, likely due to the soot derived from timber and charcoal combustion (Figure 1.2) (Camuffo et al., 2014).



Figure 1.2 Detail of Palazzo Grimani (Venice) from the painting “Grand Canal: Looking South-West from the Palazzo Grimani to the Palazzo Foscari” realised by Canaletto in 1735. Oil Painting Reproduction on Canvas. (<http://ep.yimg.com/ay/artsheaven/grand-canal-looking-south-west-from-the-palazzo-grimani-to-the-palazzo-foscari-9.jpg>)

The change in the fuel type seems to intensely influence the air pollution on urban environment because it emanates different kinds of smoke. London has experienced an interesting air pollution history because the substitution from wood to coal happened earlier, in the 13th century, than in the other parts of Europe where wood was cheap and abundant, postponing this shift until the twentieth century. In Italy, for example, timber and charcoal remained the main fuels for either domestic or craftsmen use until the mid-1800s while the employment of coal become relevant just at the end of the XIX century, during the Industrial Revolution (Camuffo et al., 2000). In London, the earliest use of coal pertained to industrial processes, such as lime-mortar production, and it was just in the late 16th century, with the diffusion of household chimneys, that this fossil fuel began to be used domestically mainly by poorer people (Brimblecombe, 2000). However, the increase in coal use has to be mainly ascribed to the Industrial Revolution (second half of the XVIII century),

when the steam engine able to produce continued rotary motion was patented by James Watt and found extensive application in driving factory machineries. For this reason, in 1700, Britain mined five-sixths of the world's coal (Wrigley, 1990). Generally, coal combustion is not particularly detrimental to buildings but this process could significantly soil built heritage in scarcity of oxygen, leading to carbon production (i.e. smoke, soot). Moreover, some combustion is only partial and produces residual or sticky pyrolysed hydrocarbons, allowing particles to adhere to buildings. In addition, several fuels contain high concentration of sulphur which, chemically transformed, could severely damage building materials (Brimblecombe, 2000). At this time, damage induced by coal was so discernible that John Thornbrough, the Dean of York Minster, suggest to desulphurise the coal in order to make it less aggressive and, in the same place during the early 1700s, black smoke and dark sulphurous crusts were removed from stonework during cleaning operations or were even pretext to demolish buildings (Brimblecombe and Camuffo, 2003).

During the Victorian period, architects paid serious attention to the right choice of construction stone to resist the polluted atmosphere. The use of complex mouldings in soft, light-coloured stone was abandoned in favour of buildings made by more resistant stone, with simpler lines and darker colours (Brimblecombe and Camuffo, 2003). Moreover, Victorian architects tried to deal with adequate actions to preserve the building materials treating stone with protective solutions, both organic (e.g. linseed oil, beeswax, resins) and inorganic (such as barium hydroxide and magnesium silicofluoride) (Brimblecombe and Camuffo, 2003). Nevertheless, increasingly smoke reduction was seen and recommended as the most suitable solution.

In the 20th century, European cities experienced a gradual decline in the use of coal that was replaced by oil gas and electricity. The so called 2nd Industrial Revolution, in effect, led to a change in the power sources. This change induced to the introduction of the photochemical smog, characterised by the interaction between organic compounds (primarily from liquid flues), nitrogen oxides and sunlight. As results, this new air pollution leads to the production of ozone, highly oxidising, and later to nitric acid and sulphate, harmful to stone building surfaces. Anyway, the potential for damage induced by sulphur-derived substances has seemed to be decreased since vehicle fuels don't release so much sulphur in the atmosphere as coal. Moreover, implemented health hazard legislation implied a fairly rapid decrease in level of sulphur dioxide, smoke and smog of the early 1950s. At the same time, the enlargement of cities and the economic growth caused a rise in the amount of vehicular traffic with accompanying emissions of nitrous oxides and black smoke particulate, different from those due to coal and oil burning. In the 1920s, the increasing request of high-performing automobiles induced to improve the existing gasoline adding tetraethyl lead, an anti-knock constituent, highly toxic. Evidence of the presence of lead, associated with Fe and Zn, is also nowadays detectable in the black crusts of most historic buildings and this is mainly derived from leaded gasoline (Sabbioni and Zappia, 1992b; Simão et al., 2006; Belfiore et al., 2013). As consequence of Pb riskiness, legislative controls on emissions lowered the amount of lead in fuel.

More recently, diesel fuel has become increasingly important in Europe. Diesel-powered vehicles have changed the composition of atmosphere yet again, emitting in the urban air large amount of particulate material that is finer and blacker than that from coal smoke in the past (Brimblecombe and Grossi, 2007). Hamilton and Mansfield (1991) reported that diesel-emitted smoke displays a soiling factor three times that for smoke from coal combustion. Black carbon is a detrimental pollutant not only for human health and cultural heritage but it performs also a warming impact on climate 460-1500 times stronger than CO₂, with disastrous consequences for the global and local weather (<http://www.ccacoalition.org/>). Diesel emissions are also richer in some organic materials and adhere as fine deposits on urban building surfaces. Therefore, this pollutant began to blacken building fabric. Simão et al. (2006) compared the particulate matter collected from the exhaust of light-duty vehicles using leaded gasoline (GPM) or diesel (DPM) as fuel. C particles are the main components in both DPM and GPM. Among these C particles, OC seems to be the principal component of GPM while EC particles prevail in DPM. Furthermore, it was also identified that unleaded

gasoline particulate matter emitted by catalyst automobiles has higher concentration of ultrafine EC than leaded GPM emitted by non-catalyst autos. Analyses of trace elements detected in the outermost portion of crusts in historic buildings (and therefore related to more recent deposition of pollutants) have also confirmed a decrease in the concentration of Pb, Fe and Zn attended by high amounts of Cu, Ni, Cr and V derived from the use of other combustibles such as oil combustible, diesel and unleaded gasoline (Belfiore et al., 2013). Regarding nitrogen oxides emissions produced in high amount by vehicular traffic, NO is not harmful to health in the amount revealed in the atmosphere while NO₂ is responsible of several environmental problems and diseases. It is proved that the NO₂ emission in the NO_x of a diesel vehicle is far higher than the proportion found in the emissions of a conventional petrol vehicle. Moreover, in new cars the emissions of NO₂ is increasingly more than those released by an old car. Thus, even if newer diesel engines remain more fuel efficient than petrol engines, their impact on air pollution is worse because of the higher emitted levels of NO_x and PM (EEA, 2016).

Even if fuel consumption is still substantial, atmospheric pollution from industrial and heating systems has now significantly decreased thanks to the improvement in the industrial combustions, the reduction of heavy petrol fractions in domestic use, the consumption of low S-content fuel and the environmental policies adopted at the local level (Ghedini et al., 2006). However, nowadays photochemical smog affects the atmosphere of many European urban sites, entailing increasingly higher concentrations of organic compounds and oxidative pollutants. Contemporary urban particulate matter displays high organic carbon/elemental carbon ratios (OC/EC), which is usually higher at the road-sides being gasoline the main source for OC (Bonazza et al., 2005). Sulphuric acid continues to be found, even with the reduced sulphur dioxide emissions detected today. Therefore, the crusts on buildings may become thinner and richer in diesel-derived carbon and organic materials. In particular, EC particles, guilty of the anaesthetic darkening of the current deposits, has increased the importance of aesthetic considerations. Additionally, biological colonization, probably enhanced by the on-going abundance of organic pollution from deposited diesel emissions, may contribute significantly to stone blackening (Viles and Gorbushina, 2003; Bonazza et al., 2007a). Thanks to Brimblecombe's research (2000), it was highlighted as many people consider that the rate of built heritage damage has become more rapid in the recent decades. In this regard, it has to be considered that an improvement in the quality of urban air has not necessarily been joined with improvements in the rate of degradation of stone materials. Indeed, damage of buildings is cumulative and the increasing citizen awareness of cultural heritage preservation has emphasised the desire for clean buildings. Nevertheless, even if most of corrosive pollutants in the urban atmosphere may well have decreased, some components, such as ozone and nitrogen oxides, still persist and may enhance the degradation of building materials or act as catalysts for traditional pollutants. In addition, the lower concentration of sulphur dioxide (phytotoxic) and the contemporary increase in particles richer in organic compounds and NO_x (nutrients) could have increased the biological degradation of stone buildings (Grossi, 2016).

Future previsions seem likely to indicate a continued reduction in sulphur emissions and probably in NO_x, with a probable general improvement in the concentration of acid deposition from the atmosphere (Brimblecombe and Grossi, 2007). The concentration of pollutants will continue to remain higher in urban environment, with the exception of ozone. The latter along with other atmospheric oxidants will damage polymers and organic materials, widely utilised in modern architecture, and may also increase the production of acids from the diminishing concentrations of sulphur and nitrogen oxides, taking part to the blackening and erosion of historic buildings. In addition to blackening, the relevant concentration of particles rich in organic compounds offers the potentiality for biological activity and oxidation processes of organic materials, thus different colouration processes (towards warmer tonality) might be expected (Grossi, 2016). Moreover, the warmer colour of deposits could be ascribed to organic carbon compounds that can be slowly converted to humic-like substances (characterised by a yellow/brown nuance), similarly to what happens in

soil (Graber and Rudich, 2006). Yellowing of buildings is increasingly yet discernable in situ, such as for the Tower of London (Bonazza et al., 2007b; Brimblecombe and Grossi, 2007). Finally, different colouration processes might be observable, depending on climate types that could also undergo variations due to climate change. Smith et al. (2011) observed that seasonality of precipitation will increase over much of the UK, implying a likely increase in the time that stone structures remain wet and possibly in the penetration of moisture. As consequence of this change, building stone in Northern Ireland has already replied through an increased incidence of algal 'greening'. On the contrary, in areas with hotter and drier summers, it might be expected the development of orange-brown or orange-grey layers derived from the colonisation of fungi, algae and bacteria, typical of Mediterranean climate (Grossi, 2016).

1.2. DIFFERENT APPROACHES FOR STUDYING DAMAGES TO HISTORIC STONE SUBSTRATES INDUCED BY AIR POLLUTION

The majority of the studies about detrimental effects of pollution on monuments are related to marble and limestone substrates because i) they have been widely employed as construction and decorative materials in different centuries all over the world, ii) their vulnerability towards atmospheric SO₂ deposition and iii) they represent a simpler system than other stones. The easiness of study is mainly induced by their good chemical homogeneity (since they are almost entirely composed of calcium carbonate) and their general low porosity that leads to well identify the interaction interface between the atmosphere and the undamaged substrate. For these reasons the present research work takes into account these kinds of stones and therefore results of the previous researches will concern principally marble and limestone.

Scientific literature offers numerous examples of international research works concerning the study of pollution impact on cultural heritage. In general, they could be classified in three major approaches:

- Analyses performed on samples collected from damaged stone portions of monuments and historic buildings. This methodology is useful to characterize the mineralogical and morphological features of pollution impact and identify the different soluble and carbon fractions deposited over time.
- Test carried out in simulation chamber in order to investigate the influence of different parameters with potential impact in degradation process, their synergistic action and the effects that occur at stone surface.
- Field exposure tests by exposing model samples to a real environment. This investigation has proved to allow a better comprehension step by step of stone damage induced by different, real and synergistic microclimatic and pollution conditions. In this way it is useful to diagnose the state of conservation of cultural heritage and address long-term sustainability of architectural materials.

The main outcomes of these researches and strengths and weaknesses of these different methodologies are described hereafter.

1.2.1. SAMPLING FROM HISTORIC BUILDINGS

The analytical assessment of damage layer and stone substrate collected by brush or scalpel from historic buildings and monuments allows to better comprehend the decay induced by atmospheric pollutants in terms of morphology, mineralogy and chemical composition making use also of several specific techniques. The knowledge of damage layer composition is therefore important to study the atmosphere-substrate interaction, identify the pollutants sources and plan restoration and conservation interventions. Macroscopic observation in situ of weathering crusts in addition to laboratory examination on samples collected from historic built heritage proved to be useful in identifying and classifying them in different classes regarding their colour, morphology, mineralogical composition, mechanical properties and water absorption characteristics. In this regard, Török and others (2003; 2004; 2008) extensively assessed features of the weathering crusts developed on oolitic limestone, widely employed as construction material in Budapest, and primarily distinguished between white crusts and black ones. Indeed, for its intrinsic characteristics, this lithotype enables the formation of not only black crusts but even of different white crusts. The latter are observed on wind and rain exposed stone surfaces and could include thick, hard white crusts and thin ones. Generally, white crusts abound with calcite (~60% in average) while the concentration of gypsum is variable and usually lower (around 27% in thick white crusts but it could reach also the 70% in thin fragile white crusts). Moreover, white crusts display also the presence of other salts and atmospheric particles related to the

prevailing environmental conditions (such as fly-ash, wind quartz, biological microorganisms and remains of the substrate - Fronteau et al., 2010), with a concentration almost constant around 11% (Török et al., 2003; 2004). A general feature of white crusts is the prevalence of calcite in the crust surface while gypsum mostly accumulates on the underside. The higher calcite concentration in thick crusts fills pores and fissures, behaving as an impermeable protective layer on the stone surface until it remains intact. On the contrary, thin white crusts undergo high permeability gypsum precipitation at the expense of calcite dissolution and therefore are affected by blistering induced by the high pressure exerted by gypsum (Török, 2003). In contrast to white crusts, black crusts appear on ashlar sheltered from the direct rain wash in a form of thick, framboidal black crusts and laminar black crusts. The first kind, known also as dendritic or globular black crusts, is usually loosely attached to the stone substrate and mainly presents as patches on protected portions of ornaments, where condensation can freely happen. Oppositely, laminar black crusts appear as thinner and more adhered to the stone surface than the framboidal ones and can completely cover building facades. As weathered, it is affected by thin scaling and blistering (Török, 2003). In both kinds of black crusts, gypsum is normally the predominant mineral (mainly in thick framboidal crusts), followed by calcite and lastly by other minerals and atmospheric particles (Török, 2003), suggesting that the dissolution does not remove the newly precipitated gypsum from the crust surface. The atmospheric particles are detected in high amount in framboidal black crusts, whose surface irregularities encourage the deposition of particles (mainly carbonaceous ones) and act as catalyst for gypsum formation. The higher the surface roughness is, the higher reaction surface entails an auto-cyclic process with new deposition of particles and thickening of the crust. Török (2003) identified that black crusts are generally more vulnerable than thick white crusts since the higher permeability of the former ones entails the formation of salts and ice crystal below and within the crust.

Measuring the mechanical properties of crusts and hosting rock, it seems that thin and thick white crusts as well as laminar black crusts evidence a higher surface strength and lower water absorption capacity compared to the stone substrate. Even if initially crusts formation could safeguard the underlying rock, their difference in porosity and strength could be responsible of crusts removal (Török et al., 2003; 2004). Moreover, taking into account the differences in porosity of the stone substrate, porous stones, like the oolitic limestone, are more prone to infiltration of a fluid and thus an accelerated damage induced by sulphation and freeze-thaw cycles in respect to less porous carbonates, such as compact limestones or marbles.

Samples collected from historic buildings could also be useful to identify the different mechanism of formation. For examples, samples of black crusts taken away from the Milan Cathedral facade look very similar by visual examination by stereomicroscopy but a careful diagnostic assessment (by Optical Microscopy – OM, Scanning Electron Microscopy equipped with Energy Dispersive X-ray Spectroscopy – SEM-EDX, Fourier Transform Infrared Spectroscopy – FTIR) allowed to accurately distinguish them into black crusts deriving from i) marble sulphation, ii) compact deposition and iii) encrustation (Toniolo et al., 2009). Even if gypsum is the main mineral recorded in all these crusts, some differences mark each typology. As described above, gypsum crusts can originate from the process of chemical acid dissolution of marble, by which calcite is transformed into gypsum under the action of sulphur dioxide and contemporarily carbonaceous particles are deposited from the atmosphere. In this case, stone substrate undergoes to chemical and mineralogical changes, entailing the stone degradation. Evidences of sulphation in process were somewhere clearly appreciable since the corrosion process starts from the boundaries of calcite grains and spreads towards the inside of crystals and pre-existent microfractures. New gypsum crystals are continuously forming at the interface marble/crust, increasing the thickness of the crust. On the contrary, in other cases gypsum comes from the outside environment, leaving sound the stone substrate on which damage layers are developed. The accumulation of exogenic materials of variable thickness, such as sea salts aerosol, atmospheric particles and remains of conservation interventions, is called deposit (<http://iscs.icomos.org/glossary.html>). The poor coherence and adhesion of these particles to the stone substrate could be overcome through solution and re-crystallisation of gypsum which acts as a binder and

brings about a compact deposit. In the case of the studied sample, the presence of a previous finishing layer on the stone substrate prevented the latter from the atmospheric corrosion, letting the underlying rock well preserved and allowing particles and gypsum deposition only from outside (Toniolo et al., 2009). Another example of gypsum crust is the encrustation, characterised by highly regular crystal organisation of gypsum derived from the crystallisation of a solution coming from an external source. Water percolation may lay, indeed, to the formation of a compact, hard, mineral outer layer adhering to the stone surface. Also for encrustation, no decay to the substrate was perceived (Toniolo et al., 2009).

The microscopic analyses of old black crusts allow even to detect the differences between old and more recent damage layers, provided that restoration interventions on historic buildings are known. Changes occurred in the combustion sources and atmospheric pollution prove to be useful tools for this investigation. In this regard, historic black crusts are characterised by layers with dendritic and inhomogeneous morphology and by the predominance of gypsum (~80-90%) with lamer/needle shape and/or microcrystalline habit (Bonazza and Sabbioni, 2016). Calcite is always detected as fragments of the hosting carbonate stone or as product of recrystallization after a dissolution phenomenon. Traces of soil dust deposition are also found as clay minerals, quartz, iron oxides and feldspar as well as soot never misses. Its presence is demonstrated by the detection of characteristic carbonaceous particles, till to 50-60µm large, deriving from coal and high-sulphur content fuels and therefore guilty of surface blackening.

According to the variation of fuels and atmospheric emissions, crusts developed from the 1950s display warmer tones (brownish-greyish) and are thinner, more coherent to the stone substrate and homogeneously distributed. As a result of the warmer tones of the newer crusts related to sulphation process, it is more appropriate to speak about “damage layers” and no more about “black crusts”, which clearly identify the appearance of older crusts. Gypsum is still present but in a lower amount and it displays a microcrystalline habit. An increase in soil dust is observed while the sub-micrometric dimension of carbonaceous particles derived from the vehicular traffic make them undetectable under the optical microscope (Bonazza and Sabbioni, 2016). Indeed, traffic proves to be the main cause of particulate pollution in urban areas of Western Europe, emitting carbonaceous particles mostly in the fine fraction, with dimension below 2.5µm. Toniolo et al. (2009) detected a lower concentration of Fe and minor compactness in the recent damage layer collected from the Milan Cathedral façade than the older one and believed that the higher transparency of newer crusts may be ascribable to the smaller amount of airborne particles.

Optical and scanning electron microscopy coupled with energy dispersive X-ray analyser allowed for recognition and classification of the different particles entrapped inside the damage layer on the basis of their morphology and elemental composition. These particles could be summarised into three main general categories:

- spherical/sub-spherical porous carbonaceous particles (soot) with circular or irregular pores with a diameter between 10µm and 60µm (Figure 1.3A). As already above-mentioned, these carbonaceous particles are the responsible for the blackening of the damage layer. They are principally emitted by vehicle exhaust, domestic heating systems, waste incineration plants, heavy industry and electric power plants that combust oil (spherical and porous particles) and distilled oil (spherical particles with irregular pores or composed of agglomerations of submicron particles) (Sabbioni, 1995; Weinbruch et al., 2014; Bonazza and Sabbioni, 2016). Moreover, carbonaceous particles from diesel emission are a complex aggregate of solid and liquid material and have a characteristic fractal appearance, as shown in Figure 1.3B. In particular, carbon particles act as core on which other components, both inorganic and organic such as heavy hydrocarbons, are absorbed and condensed forming large agglomerates. Diesel particulate matter is very fine: carbon particles have a diameter

between 0,01 μm and 0,08 μm , while the size of agglomerate doesn't exceed 1 μm , harmful for human health (<http://www.nettinc.com/information/emissions-faq/what-are-diesel-emissions>).

- Silica, silicates and /or aluminosilicate particles with a spherical, smooth and not porous surface, as shown in Figure 1.3C, found to be present in fly-ash from wood burning, coal and oil combustion and also of volcanic origin (Ausset et al., 1998; Bonazza and Sabbioni, 2016). Their coexistence with other tracers allow for determination of the specific combustion source. These particles are smaller than the previous ones (5-30 μm).
- metal particles, rare and smooth, principally composed by iron and titanium oxides and deriving from coal combustion processes (Sabbioni, 1995; Bonazza and Sabbioni, 2016), see at Figure 1.3D.

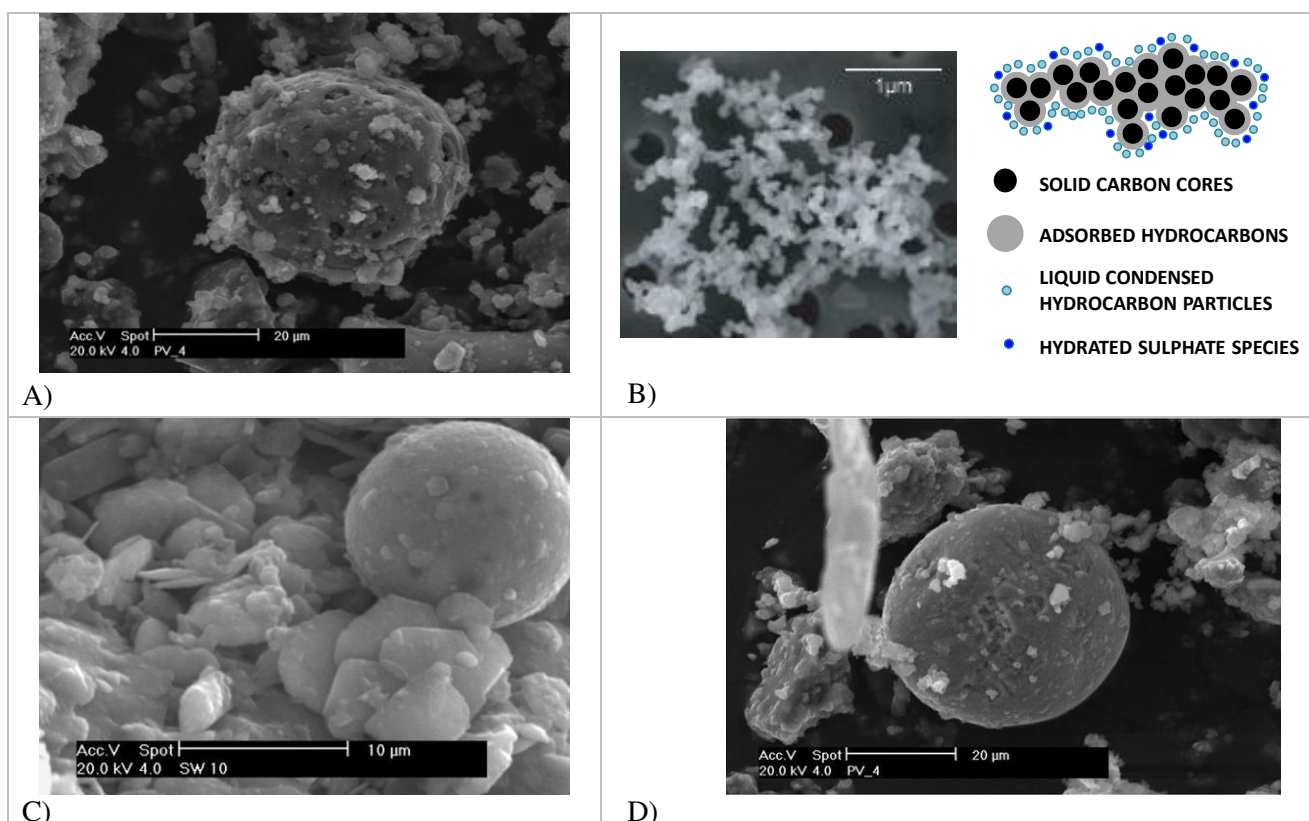


Figure 1.3 Scanning electron micrograph of: a) spongy carbonaceous particle (Nava et al., 2010); b) aggregate of soot particles (Gieré and Quero, 2010) c) aluminosilicate particle (Ozga et al., 2013); d) metallic particle (Nava et al., 2010).

In this context, it is important to cite also the accurate classification of the different components of particulate traffic emissions collected with a cascade impactor by Weinbruch et al. (2014). In general, particulate traffic emissions originate from exhaust, abrasion of tires and brakes and resuspension of road dust but in the last two decades the ratio of non-exhaust to exhaust particles has been increasing due to the exhaust emission reductions. The collected particles were categorised into 14 classes on the base of their size, morphology and chemical composition (Weinbruch et al., 2014), as described in Table 1.1, and could be a useful tool for particles discrimination on crust samples.

PARTICLE CLASSES	BRIEF DESCRIPTION
1. Traffic/exhaust	Consists of soot particles, soot particles mixed with secondary aerosol and few Pb-bearing particles. Soot particles are recognised as agglomerates of spherical C-rich particle.
2. Traffic/abrasion	Derives from tires (Zn) and brakes (Fe, Cu, Ba, Sn) abrasion or even from corrosion of vehicle parts (FeCr).
3. Traffic/resuspension	Comprises natural component (silicates and/or Fe oxide/hydroxides) internally mixed with soot or tyres/wear particles.
4. Carbonaceous/organic	C and O predominate. It may includes strongly aged soot, secondary organic particles, bitumen or tire rubber.
5. Industry/metallurgy	The presence of Fe oxides/hydroxides fly ashes (sometimes also Ti-containing) reveals the origin from metallurgical high temperature processes. These particles are characterized by a spherical morphology and by the prevalence of Fe and O as major elements.
6. Industry/power plants	Spherical silicate fly ashes are interpreted as emissions from coal power plants.
7. Secondary particles	Consists of a complex mixture of sulphates, nitrates and organic material and is found predominantly in the size range below 1 μ m. These particles are unstable under the electron beam. In detail, already Pio et al. in 1998 detected that more than 50% of fine sulphates originates from secondary aerosol production in urban area while only 4% comes directly from vehicles emission.
8. (Aged) sea salts	The principal component is NaCl but minor amounts of Mg, K, Ca and sulphate may occur within these particles.
9. Silicates	Derives from a variety of natural and anthropogenic sources. Si, O (and Al) prevail.
10. Ca sulphates	Derives from a variety of natural and anthropogenic sources. Ca, S and O as major elements.
11. Carbonates	Derives from a variety of natural and anthropogenic sources. C, Ca and O predominate but Mg could be also detected.
12. Fe oxides/hydroxides	Derives from a variety of natural and anthropogenic sources. Fe and O are the major elements.
13. Biological particles	Consists of C-rich particles while N, P, K are present as trace elements. These particles have a typical morphology and usually display diameters above 1 μ m.
14. Other particles	Comprises various metal oxides/hydroxides which could not be classified into the traffic/abrasion (different chemical composition), industry/metallurgy (different morphology) or Fe oxides/hydroxides (different chemical composition) classes.

Table 1.1 Classification of particles related to traffic emission (Weinbruch et al., 2014).

The analyses of soluble ions by performing Ion Chromatography (IC) on crusts collected from historic buildings allow to better understand the likely sources of the air pollution causing damage to built heritage. The results of different damage layers sampled in different European cities highlighted that sulphates SO_4^{2-} is always present and with high concentration (till to $540000\mu\text{g g}^{-1}$) that decreases in recent damage layers ($\sim 50000\mu\text{g g}^{-1}$) (Bonazza et al., 2005). Therefore, even if sulphation process continues to be responsible of the damage to the stone surface, its influence is diminishing. Sulphite SO_3^{2-} , revealing the occurrence of sulphur dioxide dry deposition and indicative of the contribution of the local pollution sources, is sometimes discernible but in lower amount in respect to SO_4^{2-} (Bonazza and Sabbioni, 2016).

Nitrates NO_3^- and nitrites NO_2^- , mainly originated from vehicular traffic, are measured in minor and flexible concentration. They could form very soluble salts with calcium present in the stone substrate and this water solubility as well as their inability to form stable compounds with the stone substrate may explain their small quantity found in the damage layers (Ghedini et al., 2000; Bonazza et al., 2005).

The presence of chloride Cl^- is principally detected in damage layers collected from samples located in coastal areas as it is linked to marine aerosol deposition. Moreover, chloride is also identified in urban areas due to industrial activity or near kerbs as a result of de-icing salts in cold months (Bonazza and Sabbioni, 2016).

Moreover, crusts generally include also significant concentration of small organic anions (C1-C2), formate (CHO_2^-), acetate ($\text{C}_2\text{H}_3\text{O}_2^-$) and oxalate ($\text{C}_2\text{O}_4^{2-}$). IC analyses performed on several samples of damage layers scraped from low porous calcareous stones of different monuments and building in Italian urban centres highlighted that formate, acetate and oxalate are ubiquitous and they are generally present in the order $\text{CHO}_2^- < \text{C}_2\text{H}_3\text{O}_2^- < \text{C}_2\text{O}_4^{2-}$ (Sabbioni et al., 2003). Previous research identified three main sources of these organic anions (Bonazza et al., 2005; Bonazza and Sabbioni, 2016):

1. deposition of primary and secondary atmospheric pollutants, especially those emitted by combustion processes;
2. biological weathering;
3. degradation of ancient organic treatments applied during restoration campaigns. For examples, acetates are found to derive from the oxidation of ethanol used as a solvent in protective treatments.

The contribution of these anions to the organic carbon measured in these damage layers is significant: their mean concentration is about 8% but it could reach also much higher values, as in the case of Ravenna (47%) where the industrial activities can intensify the emissions of acetate (Sabbioni et al., 2003). Moreover, these organic anions are more abundant in damage layers from stone than from mortar as well as generally higher concentration are seen in urban areas than in rural sites. However, their presence on crusts of historic buildings demands more detailed researches to better comprehend the role of these ions in monument decay. Considering the cations, calcium is usually identified in high amount as it derives from the carbonate stone substrate, soil dust and even from the use of de-icing salts in winter. Marine aerosol and soil dust are responsible for the deposition of Na^+ , K^+ and Mg^{2+} while NH_4^+ is connected to the anthropogenic activities (Bonazza and Sabbioni, 2016). It worth noting that some cations, such as Ca^{2+} , Mg^{2+} , Ba^{2+} , Zn^{2+} , NH_4^+ , can also be introduced during the chemical cleaning and consolidation processes of the stone (Přikryl et al., 2004).

Further information about the sources and also some assumption on the age of the damage layer could be acquired analysing the carbon component, since it has been identified as an important element of anthropogenic origin (for Ghedini et al., 2003, “*after sulphur, total carbon is the main anthropogenic component of atmospheric deposition present in damage layers on buildings*”). The carbon present in the damage layers of historic buildings and monuments could derive from (Bonazza and Sabbioni, 2016):

- calcium carbonate, originating mainly from the stone/mortar substrate on which the damage layer has developed;
- deposition of atmospheric particles as primary and secondary pollutants;
- biological weathering induced by the action of microorganisms. As abovementioned, some biological organisms are able to produce oxalic, acetic and formic acids, which react with the substrate, resulting in calcium oxalate, acetate and formate;
- surface treatments employed in past restoration and conservation interventions, such as wax, oil, protein, etc.

Analyses performed on damage layers highlighted that the total carbon component (TC) could be summarised in non-carbonate carbon component (NCC) and carbonate carbon fraction (CC). The initial researches aimed to discern and measure the TC and NCC fractions, using two opposed methodologies (Bonazza and Sabbioni, 2016):

- combustion and IR technique performed on bulk sample allow to measure TC while CC is evaluated by differential and gravimetric thermal analysis (DTA-TGA). The NCC is then obtained by subtracting CC from TC;
- after the sample has been kept in an atmosphere saturated with HCl in order to eliminate the CC, the NCC fraction is measured by combustion and IR technique while CC by DTA-TGA. TC is thus got from the addition between CC and NCC. This methodology proves to provide more accurate results, as reported in the examples cited by Bonazza and Sabbioni (2016) concerning the analyses of black crusts collected from marble and limestone monuments in different Italian cities. Moreover, it showed that NCC portion decreases from the external surface towards the inner part of the damage layers, confirming that stone almost does not contribute to the NCC value.

Excluding the carbon deriving from the carbonate substrate (CC), the remaining portion (NCC) is composed of elemental carbon (EC) mainly due to combustion processes and organic carbon (OC), of both primary or secondary natural and anthropogenic origin (Ghedini et al., 2006). The latter constitutes a complex system, as the organic materials detected in the damage layers derive not only from the deposition of carbonaceous particles but also from the adsorption of volatile organic compounds over the already deposited material. In order to measure the OC and EC concentrations in atmosphere investigations, several methodologies are usually utilized. Apart from the not frequently adopted photo-acoustic methods for quantify the aerosol elemental carbon, optical methods, in reflectance or transmittance, are used to evaluate the dark component of carbonaceous materials while thermal oxidation and thermal-optical, in transmittance and reflectance, are useful for analyzing atmospheric carbonaceous particles. Nevertheless, further investigations were necessary because of i) lack of clarity regarding the meaning and the differences of the terms black carbon, soot, graphitic and elemental carbon, dark component of carbonaceous aerosol, that render the obtained data unfit for comparison, ii) disagreements about methodological parameters and iii) the fact that carbonate carbon, negligible in the atmospheric aerosol, has to be precisely identified in the analysis of a damage layer since it represent almost half of the total carbon in black crusts (Ghedini et al., 2000). The OC/EC quantification in the damage layers is rather complex as the technique usually employed to analyse them in PM (i.e. thermal optical transmittance method) cannot be successfully used because it requires the homogeneous deposition of powder sample on quartz fibre filters. Therefore, Ghedini and others (2000, 2003 and 2006) developed and improved a new methodology to detected and quantify TC, CC, NCC, EC and OC by flash combustion/gas chromatographic analysis using a carbon-hydrogen-nitrogen-sulphur-oxygen analyser (CHNSO EA 1108 FISON Instruments), thanks also to the support of EC Project “Carbon content and origin of damage layers in European monuments–CAMEL” (EVK4-CT-2000-00029). The analysis requires about 1 g of material

and comprises three principal steps performed on a different part of the same damage layer specimen, previously ground (Ghedini et al., 2006):

1. TC is quantified by burning one part of the bulk sample.
2. NCC is measured by the combustion of a second part of the sample after carbonate decomposition by means of HCl vapours and the complete removal of CO₂, HCl and H₂O after the permanence in a KOH drier. CC is then calculated as the difference between TC and NCC.
3. EC is detected by oxidation of the residue obtained from a series of alternating basic and acid treatments at different temperatures in order to eliminate inorganic matrix and organic compounds. OC derives from the subtraction of this final value from NCC.

This methodology proves to satisfactorily distinguish and measure the carbon fractions of damage layers even if a decreasing in the required amount of sample is needed as not always damage layers provide such a big quantity of analysable material. Literature provides also other methodologies to study the carbonaceous fraction present in the damage layers. For instance, Fermo et al. (2015) proposed a new method that requires less material to analyse (just 2 mg) in respect to the analysis proposed by Ghedini et al., (2006). First TC is determined by a carbon-hydrogen-nitrogen (CHN) analyser from one part of the sample. Simultaneously, OC is removed by combustion and the residue analysed by CHN analyser to detect EC+CC. Extracting CC from the ionic balance, EC could be calculated by difference as well as OC: $OC = TC - (EC + CC)$.

The analysis of samples of damage layers collected on historic buildings in different European cities highlighted a general prevalence of OC in respect to EC (Ghedini et al., 2000; Bonazza et al., 2005; Ozga et al., 2013; Ghedini et al., 2006). This trend is particularly pronounced in the damage layers sampled from the monuments sides exposed directly to air pollution induced by vehicular traffic and confirms also the results of monitoring campaign of aerosol measured in different European cities. However, there are also some exceptions as in the case of damage layers collected in Milan and in some specimens also from Venice, where EC dominates OC (Bonazza et al., 2005; Ghedini et al., 2006; Fermo et al., 2015). A possible explanation is the evolution of the deposited powder to a more cohesive crust (Fermo et al., 2015) or more likely the consequences of emissions released from industrial activity (Bonazza et al., 2005). These cities are indeed located in the Po valley, known to be the most industrialised area of Italy. Moreover, the use of coal and oil combustion for domestic heating and industrial purpose could have enlarged the EC concentration as the scarce efficiency and the combustion at relatively low temperatures, characteristic of the early industrial era, can increase the EC emissions.

Finally, a general correspondence between the OC amount detected in the damage samples and the age of black crusts was observed and introduced by Bonazza et al. (2005) because higher OC fraction was detected in more recent damage layers. Nevertheless, it is important to consider that OC compounds could have been decomposed during time and thus are more hardly detected in ancient damage layer as well as the current increase in biological activity could explain the present excess of organic matter (Bonazza et al., 2007b).

Further information useful to discriminate between old and modern damage layers as well as identify the major combustion sources could be acquired by geochemical characterisation of the damage layers (Bonazza and Sabbioni, 2016). The presence of some heavy metals and other elements is in fact a distinctive element of some sources. For instance, Pb, Fe and Zn, commonly detected in the inner portion of black crusts, could be linked to the use of leaded gasoline while S and V are diagnostic of domestic heating and S of coal combustion.

There are different techniques able to characterize the different chemical elements present in the damage layer as laser-induced breakdown spectroscopy (LIBS) and atomic absorption spectroscopy (AAS) but recently inductively coupled plasma mass spectrometry (ICP-MS) gains influence as this sensitive technique is capable to analyse a high number of trace and rare earth elements (REE) on bulk sample, unfortunately

without detecting the geochemical variations between crust, altered and unaltered substrate (Barca et al., 2010). The distribution of Rare Earth Elements, which has increased exponentially in the last fifty years, is suitable to tracing the origin of certain particles. A further improvement of this technique with the addition of laser ablation (LA-ICP-MS) has led to investigate a great number of elements in a short time span and using small amounts of sample (with spot resolutions of about 40-50 μm), allowing the determination of micrometric compositional variations (Belfiore et al., 2013). In this way, it is possible to better understand the major stationary and mobile combustion sources responsible of the damage to architectural surfaces over time as well as to obtain the profile of trace elements from the inner layers to the external ones. Analyses of different specimens of damage layers samples from different European historic buildings show that the concentration of heavy metals in the crusts is higher than those in the substrates, mainly for Fe, Pb, Zn, V, Cu, Cr, Sb and Ni. Among these elements, Pb, Fe and Zn are mainly recognised in the inner portion of the crusts (probably pertaining to the oldest deposit and due to the use of lead gasoline) while their concentration decreases in the outermost part of the crusts together with high amounts of Cu, Ni, Cr and V explicative of the change in combustibles use as gasoline, oil combustible and diesel. The different height of sampling influenced the results, too: architectural surface located close to the ground (2-5 m) are characterised by higher amount of heavy metals relative to the influence of vehicular traffic (e.g. Pd, Zn, Cu, Sn) whereas at higher height (about 40 m) the background pollution from stationary combustion sources (i.e. industries and domestic heating) are the major source of Fe, V, As and Cd (Belfiore et al., 2013; Bonazza and Sabbioni, 2016). Furthermore, it cannot be excluded that the aforementioned elements can be linked to polychromy of stone surfaces as well.

Nevertheless, it is not always easy to distinguish if a measured element comes from stone substrate rather than from the deposition of atmospheric gas and aerosol. In order to solve this problem, the enrichment factor (EF) could be calculated as follow:

$$EF_{carb}(X) = \frac{\left(\frac{X}{Ti}\right)_{black\ crust}}{\left(\frac{X}{Ti}\right)_{carb.\ rock}}$$

where X is the concentration of the investigated element, Ti the concentration of the indicator element in the black crust and carbonate rock, respectively (Sabbioni, 2000). Ti was selected as reference element because it is not linked to neither black carbon nor carbonate rock. The elements having an EF lower or close to 1 have to be attributed to the carbonate substrate while in the case of values higher than 1 these elements come from the atmospheric deposition and therefore are strictly related to the black crust. Analysing samples collected in several Italian urban sites Al, Mg, Si, K, Fe, Ni, Mn and Sr are often ascribable to the stone substrate while S, Cl, Na, Cu, V, Zn, Br, Pb have non-stone origin (Sabbioni, 2003). Moreover, this equation is also useful to discern whether the components participating in the formation of the damage layers belong to natural or anthropogenic sources. Considering that soil dust is the main natural source, the equation is calculated for soil dust, which replaces the carbonate stone at the denominator:

$$EF_{soil\ dust}(X) = \frac{\left(\frac{X}{Ti}\right)_{black\ crust}}{\left(\frac{X}{Ti}\right)_{soil\ dust}}$$

Si, Fe, Al, Na, K and Mg usually identify soil dust as their major origin while S, C, Pb, V, Sr, Zn, Ba, Cu and Ni are related to an anthropogenic cause.

1.2.2. TEST CARRIED OUT IN SIMULATION CHAMBER

A method to address the effects of air pollution on stone decay combines detailed investigations of weathered building materials sampled in polluted urban areas with specific experiments under controlled laboratory conditions. Simulation chambers, employed since the 1970s, are useful tools to better assess the environmental parameters (e.g. temperature, relative humidity, gas and particles) potentially responsible for the premature ageing of building materials, their synergistic action and the consequences they may cause to historic buildings and monuments. Regarding stone conservation, environmental chambers have been widely used to test the effects of specified environmental/climatic conditions on materials in order to better understand the damage induced by natural weathering to stone substrate on varying qualitatively and quantitatively the environmental parameters as well as to assess preliminarily the efficiency of conservative products applied on building materials by performing accelerated-aging tests (Doehne and Price, 2010).

More complex is the study of pollutants deposition as attention has to be paid to many parameters concerning climatic parameters, pollutants and material features. These influences could be analysed individually, by varying only one parameter at a time, or in synergy in order to simulate more complex chemical environment. Moreover, simulation tests on stones have been carried out utilising both static and flow climatic chambers for controlling the temperature and humidity with different particles and gas concentration. However, the research in this field is not simple as to ensure quantitative results in relatively short time, these laboratory tests are performed under extreme environmental conditions which are usually far from the reality and the amount of detailed results is limited and heterogeneous for instrumental limitations. Furthermore, the extreme variability of environmental parameters occurring in the real world as well as stone-related properties represent still a challenge to be reproduced experimentally. On the other hand, these chamber tests could give an improvement in the knowledge if they are used to study any single component of complex problems that threaten the conservation of built heritage, such as the sulphation of carbonaceous stones, as long as you keep in mind that the reproduced model is only a simplification of the reality and thus the results have to be combined with those deriving from real samples or field exposure tests.

One approach to define the key physical and chemical parameters responsible of the sulphation phenomena has been, indeed, to perform controlled laboratory simulation, starting from evaluating the effects of exposure to SO₂. In this regard, several factors were found to influence the rate deposition of SO₂ (Sabbioni, 2003):

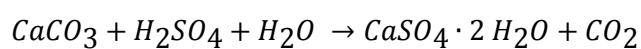
- concentration of SO₂. SO₂ deposition was calculated indirectly by measuring the decrease in gas concentration in the chamber where test samples were exposed or quantifying the amount of material deposited on the specimens (Sabbioni, 2003 and related references). Nevertheless, experimental errors took place in both cases as SO₂ could be deposited also to chamber walls and too long exposure periods as well as big SO₂ concentration were required, respectively. For instance, too high SO₂ concentration may alter the pH of the surface water films slowing the formation of sulphate and thus promoting the development of sulphite (Massey, 1999).
- Presence of oxidants, such as NO₂ and O₃, as catalysers of the oxidation of the absorbed species containing four-valent S or CaSO₃ to sulphate. In literature there are many examples of researches performed during the 1980s and the 1990s on the catalytic role of NO₂ that provide controversial results (Sabbioni, 2003). However, Chabas et al. (2015) lately confirmed that the SO₂-carbonate interaction is enhanced by the presence of NO₂ and even more by O₃, which act as catalyser, but always in conditions of 90% of relative humidity. Previously, Elfving et al. (1994) highlighted nonetheless that NO₂ requires moisture to be present to sulphate formation on prepared surface sulphite on calcite while O₃ reacts rapidly both at dry and humid conditions. It has to be mentioned

that this sulphite-sulphate transformation seems to occur at the surface of the calcite and not in the gaseous phase.

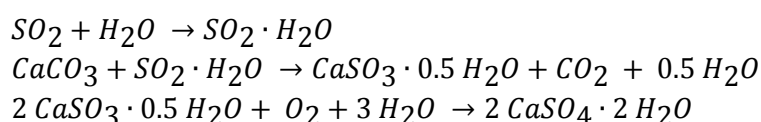
- Humidity. Serra and Starace (1978) highlighted that a humidity value around 90% is essential for the progress of the corrosion reaction. This influential factor is proven also in a more recent paper (Chabas et al., 2015), where small gypsum efflorescences are always present in the intercrystalline space between micrometric calcite grains, which is the typical location of the last desorption zones likely characterised by longer time of wetness and where the residual multilayers of water remain. In this regard, Brimblecombe et al. (2006) and Bonazza et al. (2009) declared that the deposition of pollutants on building materials is influenced by the time of wetness that is the time fraction during which building surface is covered by a thin layer of water. This is possible because gas, such as SO₂, is soluble in water as well as particles can be deposited more effectively on wet surfaces. It is possible to assume as time of wetness the period when relative humidity is > 80 % and water is in liquid state (T > 0°C).
- Stone features, as rough and porous limestone absorb more SO₂ than polished marble. Moreover, also the chemical composition, homogeneity and porosity of stone influence the sulphation phenomenon.

The results achieved by many simulation chamber tests (see Sabbioni, 2003 and related references) identified two possible mechanisms for the sulphation of carbonate stones:

1. the direct formation of gypsum from the interaction between calcium carbonate and sulphuric acid, in presence of humidity



2. the formation of calcium sulphite hemihydrate, as an intermediate stage, followed by the oxidation into calcium sulphate dehydrate



Moreover, literature reports also investigations on the relationship between atmospheric aerosol and sulphation process. Ausset et al. (1996) assessed the behaviour of a oolitic limestone, either i) naked or covered with ii) fly ash from a French power plant that utilizes heavy fuel oil or iii) soot particles corresponding to the combustion products of exhausts of diesel motors in polluted urban areas, exposed for one year to the same environmental conditions (temperature, relative humidity and SO₂ and NO₂ concentrations) measured in Milan urban area. The concentration of pollutants as well as the value of climatic parameters are important elements to be considered in these simulation tests as they are very often emphasised to better study a certain phenomenon, even if they move away from reality. During the first months, SO₂ deposition velocity was higher on naked stones while later it increased in sample covered with fly ash. In general, the experiment showed that SO₂ deposition velocity decreases in all cases with time and, considering the two different coverings, soot particles seem to play an important screening role while fly ash is found to play an active role in fixing sulphur compounds on stone.

Furthermore, many simulation chamber tests have dwelled mostly on the importance of carbonaceous particles of black carbon in atmospheric SO₂ oxidation. The discussion topic for long was the comprehension whether the catalytic effect should be attributed to the chemical composition of the particles (heavy metal content) or to their high specific surface area. For this reason, Sabbioni (2000) scattered aerosol particles

derived from oil-fueled combustion sources and carbonaceous particles not present in real atmospheric aerosol (activated carbon and graphite) onto carbonate stones specimens. The presence of aerosol particles enhanced the SO_4^{2-} formation in respect to blank samples while the other two kinds of particles did not increase sulphation phenomenon. Therefore, the heavy metal content of carbonaceous particles (mainly Fe) contributes significantly to the sulphation of calcareous materials, producing chemical and physical damage to stone monuments and historic buildings. This work confirms the results emerged from a previous research (Sabbioni et al., 1996) where aerosol used to cover stone samples was collected from a centralized domestic heating plant (P1) and electricity generating stations (P2 and P3). The highest SO_4^{2-} concentrations were found for the P2 particles, not influential for their specific surface but for their heavy metal content, particularly iron. The role played by carbonaceous particles in the heterogeneous oxidation of SO_2 into SO_4^{2-} is basically catalytic on account of their heavy metal content while the role of specific surface is limited. Moreover, SO_3^{2-} formed by interaction between SO_2 and stone was also quantified, highlighting the hindering effect of carbonaceous particles in SO_3^{2-} formation. Finally, the authigenic nucleation of gypsum crystals by carbonaceous particles was proved to be negligible (no more than 0.04%) in respect to the total gypsum formed by SO_2 -stone interaction (Sabbioni et al., 1996).

Recently, Chabas et al. (2015) developed a new experimental chamber (CIME) for simulating the interactions between materials of the cultural heritage and the environment. In addition to usual climatic parameters and gaseous pollutants, CIME has introduced the possibility to control the injection of particulate matter such as marine aerosol, soot and terrigenous particles. During the injection phase of the only soot particle deriving from the combustion of propane in order to simulate diesel soot, these are distributed in a unimodal size distribution, centred on 143 nm. After settling, their number concentration decreases because of their deposition and clustering of air-suspended soot particles, confirmed also by the doubling of principal size distribution. Adding materials of cultural heritage in the simulation test, first experimental results on the effects of the deposition of soot particles highlighted how soot increases the roughness of glass and Carrara marble (very low at the beginning) while the roughest tested sample (limestone of Saint-Maximin - biocalcarenite) reveals no differences before and after particles deposition, probably due to the strong adhesion of soot on all surfaces, also inside the open porosity.

The impact of air pollution on stone buildings and monuments is related to the deposition and accumulation of pollutants on their surface through mechanisms that happen both in dry and wet conditions. Therefore, it is important to better understand the quantity of pollutants deposited on the stone substrate in respect to their concentration in the atmosphere. In this regard, simulation chamber as well as wind tunnel experiments proved to be useful instrument for detailed assessment of the issue.

Although the rate of dry deposition of pollutants to surfaces is variable and depends on several parameters (see hereafter), dry deposition is a continuous process leading to the continuous formation of reaction products (e.g. sulfates and nitrates) on the stone surface. Dry deposition is connected with the deposition flux F of pollutants, i.e. the mass of pollutants per unit time and area to the surface ($\text{g cm}^{-2} \text{s}^{-1}$), and it is commonly expressed by the deposition velocity v_d (cm s^{-1}), directly proportional to the deposition flux and inversely correspondent to pollutant concentration C (g cm^{-3}):

$$v_d = \frac{F}{[C]}$$

However, the dry deposition of a pollutant is influenced by aerodynamic factors and it has to be considered as an irreversible phenomenon by chemical reaction or physical processes as dissolution or absorption. Therefore, the deposition velocity of gases could be also defined as the inverse of the sum of the atmospheric and surface resistances (Sabbioni, 2003):

$$v_d = \frac{1}{r_a + r_b + r_c}$$

where r_a , r_b , and r_c are the aerodynamic resistance (function of wind speed and air turbulence), the quasi-laminar boundary layer resistance (depending on molecular diffusivity and turbulence), and the surface uptake resistance, respectively. The latter is a function of the chemical and physical properties of the surface and thus of chemical composition of the surface, surface roughness, porosity and surface moisture. Consequently, SO₂ dry deposition velocity differs for different lithotypes utilized as building materials in response to their r_c , as the examples reported by Sabbioni et al. (2003). Carbonate materials, characterised by acid-buffering capacity, show to have a low resistance to SO₂ dry deposition and so a relative high SO₂ v_d in respect to silicate stones. In particular, a compilation from literature of SO₂ dry deposition velocity on Carrara marble evaluated from chamber test experiments at different exposure conditions (Pantani et al., 1998) highlighted that v_d increases with relative humidity, wind intensity and also adding O₃ and NO_x in the chamber test atmosphere while it results overall constant by injecting more SO₂.

For particles, the deposition flux depends on the concentration of particles in the air and on their deposition velocity; the latter is strongly connected with their size. As presented in Nicholson (1988), very small particles (i.e. those with a diameter below 0.1 µm) are controlled by Brownian motion that allows rapid movements across the viscous air layers above the surface while gravitational sedimentation prevails for coarse particles (i.e. with a diameter more than 1 µm) and thus the “terminal” (or gravitational settling) velocity v_t (v_g) increases with particle size. More difficultly quantified are the intermediate size particles, affected by impaction and interception phenomena. In addition to these predominant circumstances, the presence of phoretic effects (diffusiophoresis, thermophoresis and electrophoresis) could complicate the already complex situation.

Deposition velocities have been determined by different authors (see Watt and Hemilton, 2003 and related references) but results report different values depending on the assumed experimental conditions.

Overall, some difficulties are observed in comparing the results obtain by simulation chambers because the high liberty supplied to researchers by the experimental equipment implies the possibility to chose different values of experimental parameters, which sometimes are also emphasised to better study a specific phenomenon.

1.2.3. FIELD EXPOSURE TESTS

The uncertainty of the results about damage of building materials obtained by simulation chamber and the difficulties to experimentally reproduce both intrinsic (stone-related properties) and extrinsic (environmental-related variables) factors has led the researchers to perform field tests in order to assess the state of conservation of cultural heritage and address long-term sustainability of architectural materials. Surrogate materials with similar composition to the material present in the cultural heritage are mounted in a rack and exposed outdoors in the vicinity of the building/monument of interest. The substitute surfaces passively receive the gaseous pollutants and particles and could be used for long-term integrative sampling. This approach of study is useful to better identify and observe the effects of the exposure of stone to different real environmental conditions and provides true assessment because field trials replicate the complexity of pollution deposition to actual objects, which depends on many parameters such as pollutants concentration, particles size distribution, wind speed, turbulence and surface characteristics of the object. Moreover, in comparison to conventional particles sampler, this methodology is silent, does not need electricity and can be performed inconspicuously and without the regular presence of technical personnel.

Literature provides several examples of the exposure of quarried stones to real environment mainly to study the processes affecting the dissolution of rain-washed stone in the environment (Sabbioni et al., 2003 and related references). For this purpose, samples are exposed outdoor to the direct impact of rain and after several months the physical-chemical and aesthetic properties will be analysed. Moreover, in conjunction with these studies, stone samples have been very often located outdoor in (partially) sheltered conditions to assess the effects of pollutants on building materials. This approach allowed for better recognition of the pollution influence mainly on sheltered samples and only partially to the exposed ones when pollutants are dissolved or washed out by precipitations.

During the 1980s, the United Kingdom recommended researches to assess the present and potential problems related to the degradation of building materials and to evaluate the rate of decay attributable to actual pollution and to natural weathering. In this regard, the Buildings Effects Review Group was established and worked on the National Materials Exposure Programme (N.M.E.P.), run from 1987 to 1995. At the time, one of the most important problems to face was to determine if rates of buildings degradation have changed as a consequence of the reduction of concentration of SO₂ and black smoke during the last 30 years and the concomitant increase in NO_x concentration. Therefore, small samples of different building materials (i.e. stones and metals) were exposed in 29 sites in United Kingdom for a minimum of 4 years till to 8 years and their features analysed after 1, 2 or 4 years (Yates et al., 1988). Simultaneously, meteorological conditions (i.e. temperature, rainfall, rainfall pH, relative humidity, wind speed and wind direction) and atmospheric pollutants (NO₂ and SO₂) were collected from all the sites for the duration of the exposure programme. In particular, Viles et al. (2002) analysed stone samples (tablets of Monks Park and Portland limestones) exposed in sheltered and unsheltered conditions in United Kingdom (at Wells, Bolsover and Lough Navar, characterised by different air pollution concentration, rainfall amount and pH) for 1-, 2-, 4- and 8- year periods by means of colorimetric analyses, optical microscopy, scanning electron microscopy and ion chromatography (Figure 1.4). The most polluted site studied displayed the highest rate of surface recession, soiling of sheltered samples and soluble salts content. The identification of pollution-derived particulates also



Figure 1.4 The National Materials Exposure Programme site at Bolsover Castle, Derbyshire (Yates et al., 1988).

confirmed soiling mainly related to the accumulation of airborne particles in absence of rain. On the contrary at the other two sites, exposed samples became soiled more quickly than sheltered ones and more microorganisms were found on unsheltered samples, suggesting a biological origin of the darkening. Furthermore, attention has to be paid also to the position of stone carousel as in the case of specimens located in York (Butlin et al., 1995). In this case study, the movement of already exposed samples to a more unsheltered position appeared to give greater exposure to wind driven rain onto the “sheltered” samples and might explain the decrease in weight gain attributable to sulphation after a previous increase.

Contemporarily, the United Nations Economic Commission for Europe (UNECE) started working to gradually reduce and prevent air pollution and acid rain responsible of health problems and damage to historic buildings, monuments and ecosystems. In this regard, in 1979, the Convention on Long-range Transboundary Air Pollution was signed to address this hazard and working groups called “International Cooperative Programmes” (ICPs) were set up to organise the research and monitoring activities in a specific field. Among the others, in 1985 the “International Co-operative Programme on Effects of Air Pollution on Materials, including Historic and Cultural Monuments” (ICP Materials) was established. The latter aims to quantitatively evaluate the effects of sulphur and nitrogen compounds in combination with the other major air pollutants and climate parameters on several materials, including also those used in objects of cultural

heritage, and to assess the trends of corrosion and pollution (<http://www.corr-institute.se/>). This quantitative assessment is useful to determine dose-response relationships as well as to evaluate acceptable and/or target levels and to calculate costs attributed to material damage. In order to achieve these goals, field exposure tests have been planned in about 30 exposure sites across around 18 countries of Europe, North America and Middle East, with some changes over the years. The first phase of ICP Materials (1987-1995) was focused on acquirement of long-term data on corrosion and pollution in order to develop dose-response functions (Tidblad et al., 2012). At that time, SO₂ concentration was still high but decreasing and therefore a new campaign was necessary to quantify the effects also of incoming pollutants such as HNO₃ and particulate matter (multipollutant exposure – 1997-2001). In this regard, an EU project (FP7 MULTI-ASSESS Project – EVK4-CT-2001-00044) started in 2002 for an extensive measurement and study of the corrosive and soiling effects of particulate matter and nitric acid, exploiting the already existing exposed set-up of ICP Materials. Later, the work of ICP Materials focused on the assessment of stock of materials at risk in collaboration with the 2004–2007 EU 6FP CULT-STRAT project on management strategies that led to edit a manual on the effects of air pollution on materials and cultural heritage (Watt et al., 2009). These results are useful to perform a complete evaluation of cost savings and introduce the concept of tolerable corrosion/soiling and pollution levels for indicator materials. Small samples of different materials utilized in the cultural heritage, including structural metals, stone materials, paint coatings, electric contact materials, samples of medieval stained-glass windows and polymer materials, have been exposed in different site for different lapses of time. A demonstration of the exposure setup located in Prague is reported in Figure 1.5. Taking into consideration stones, samples of Portland Limestone and white Mansfield dolomitic sandstone were exposed for the 8 years of the original exposure (1987-1995) both in sheltered and unsheltered conditions. Only the limestone was later exposed in sheltered/unsheltered conditions (1997-1998, 1997-1999, 1997-2001, 2002-2003) and in uncovered situation (2005-2006 and 2008-2009) (Tidblad et al., 2012). Finally, a further exposure of 4 years (2011-2015) was planned to evaluate long-term corrosion trends attributable to atmospheric pollution on carbon steel, zinc, aluminium, weathering steel and limestone in unsheltered conditions and soiling of sheltered modern glass (Tidblad et al., 2016).



Figure 1.5 Field exposure test of samples within the ICP Materials – Prauge, 2009 (<http://www.corr-institute.se/>).

From the beginning of the exposure, the average SO₂ trend relative to the year 1987 shows a decreases ceased during 2000 and 2006 with a slight concentration loss during 2008-2009 as well as NO₂ continuously decreased during the period 1987-2009 while O₃ concentration remains constant after a first increase during the 90's (Tidblad et al., 2012). Furthermore, the measurement of HNO₃ and particulate NO₃⁻ resulted very important as very reported measurements were present in urban areas of Europe and elsewhere but the strong acidity of nitric acid and the high hygroscopicity of the related salts make them particularly harmful and corrosive for cultural heritage materials. This hazard is particularly relevant since nitric acid is rapidly absorbed on most surfaces and has a very high deposition velocity. Analysing the measurement campaigns, nitric acid concentration decreased on the average about 20% per

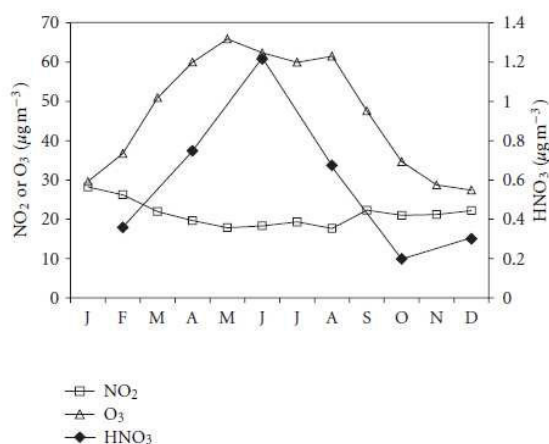


Figure 1.6 Seasonal cycle of nitric acid and two of its precursors during 2008/09 (Tidblad et al., 2012).

3-year period as well as the concentration of their precursors NO_2 and O_3 (Tidblad et al., 2012). A similar result was detected also for particulate nitrate. Moreover, the comparison of the concentration of HNO_3 , NO_2 and O_3 against the latitude and the average seasonal variation proved that the most important formation process of HNO_3 was the photochemical formation that happens in the daytime thanks to the reaction between OH radicals and NO_2 , abundantly emitted also by the modern diesel engines. A similar seasonal trend of HNO_3 and O_3 concentration showed also a maximum during the brightest time of the year and minimum during the darkest one, as reported in Figure 1.6 (Tidblad et al., 2012). Generally, the HNO_3 amount resulted higher in the urban areas than the rural sites.

Generally speaking, limestone decay seems to have been decreased compared to level measured in 1987 but no average trend among the test sites was possible. As regard the development of dose-response functions, a discussion of the most important results will be proposed in the next subchapter.

Regarding the far East Asia, the Committee on the Cultural Properties and Materials Damage by Air Pollution was established in 1993 by the Air Pollution Subcommittee of the Japanese Society for the Atmospheric Environment with the aim to evaluate the effects of acid deposition on cultural heritage cultural properties. In this context, samples of bronze, ancient copper, pure copper, steel and marble were exposed in 17 test sites (5 in China, 10 in Japan and 2 in Korea). Two sets of specimens were separately exposed to both unsheltered and rain-sheltered outdoor conditions, which were collected and analysed after 3 months and 1, 2 and 4 years of exposure. Kim et al. (2004) provides the information on the 1-year average corrosion rates of the test materials. For marble, the corrosion rate of marble in the unsheltered conditions was more than six times larger than in the rain-sheltered conditions, highlighting the wet acidic deposition as the most dangerous responsible of damage. As steel showed to be very sensitive to air pollution, it proved to be a good indicator for evaluating the material damages due to air pollution.

The problem of soiling of building stones in urban environments was accurately studied by Grossi et al. (2003) by performing ad hoc exposure of samples (5 x 5 x 1 cm) of marble, granite, limestones and dolostone in Burgos and Oviedo, characterised by Continental and Atlantic climate, respectively. The samples were exposed outside in both sheltered and unsheltered conditions for a period between 7 and 12 months. A darkening of limestones and marble specimens both sheltered and unsheltered (mainly in the covered ones) was detected in the couple of exposure sites while no relevance in soiling was detected in granite samples. The differences between stone in the inclination to soiling were proved to be more related to surface roughness than to stone porosity: a rough surface is able to easily trap atmospheric particles in respect to a stone with larger pores on the surface. Moreover, the absolute variation of reflectance is more evident in lighter stones as well as a wetter and windier climate could increase the washing out of deposited particulate.

Another experimental examination on black soiling of architectural limestone was carried out by Urosevic et al. (2012) by exposing samples under Granada urban conditions for 2 years. The samples (10 x 10 x 2 cm) were located outdoor, only vertically, in areas exposed to high or low pollution. The morphological and compositional analyses performed with Environmental Scanning Microscope (ESEM), SEM-EDX, Transmission Electron Microscopy (TEM) and micro-Raman Spectroscopy highlighted the presence on all samples of carbon-rich particles, both organic and inorganic (attributable as soot particles) and mixed with clay minerals. Fewer amounts of highly porous Na and Cl particles, mineral dust particles as well as evidence of biological colonization were detected. Additionally, it should be noted that rain-sheltered areas proved to be more suitable for gypsum crust formation. Regarding the soiling process, all samples underwent a general decrease in lightness (i.e. blackening) and an increase in the chromatic parameters a^* (i.e. towards red) and b^* (i.e. towards yellow), mainly in those samples exposed in heavy polluted sites, causing a colour change perceptible by human sight. This colour variation seems to be more pronounced in unsheltered

samples that after exposure were characterised by a higher surface roughness than sheltered surface, fostering more intense differential erosion and in turn triggering black soiling.

At national level, some examples of field exposure tests concerning the effects of pollution on limestone and marble are available. With the purpose of verifying the correlation between stone decay and pollution, Realini et al. (1995) exposed Carrara marble samples in Milan and Aosta, cities characterised by different industrialisation levels, population densities, traffic intensities and hence environmental conditions. Plaques of marble (5 x 5 x 2 cm) were exposed outdoor for two years, inclined at 45 degrees towards the north, in a partially sheltered condition that protected them from precipitations but allowed the deposition of particulate matter. Every 6 months (corresponding to the cold and warm periods, respectively) samples underwent gravimetric, colorimetric and chemical analyses. Concerning the results of the chemical analysis of the soluble fraction of the powders extracted by immersion in ultra pure water, an increase of sulphate and nitrate during the cold period was measured, likely due to the influence of heating systems. The amount of particles deposited on the surface area of samples highlighted a continuous growth, higher in Milan than Aosta and interrupted only by a violent storm that partially wetted and removed a small amount of particulate matter. This trend of particle deposition influenced also the surface blackening: sample exposed in Milan were subjected to a higher fall in luminous reflectance due to the carbonaceous particles present in the PM. Moreover, the Authors tried also to calculate and quantify a decay parameter from the outcomes of chemical and gravimetric analyses, displaying an increase in decay in parallel to the exposition period.

Zappia et al. (1998) exposed small samples (10 x 10 x 5 mm) of stones (Carrara marble, Travertine, Trani and Portland limestones), along with mortars (lime, pozzolan and cement mortars), in areas unsheltered, sheltered, and partially sheltered from rain wetting. Samples were placed in the city centre of Milan to simulate the characteristic environment of a large industrial area and Ancona, as example of example of a maritime site. After 6, 12 and 24 months samples were analysed by ion chromatography, X-ray diffraction and SEM-EDX. Sulphation process was detected as the main degradation process affecting both stones and mainly mortars. Chromatographic analyses detected the presence in all samples of sulphate and sulphite, as an intermediate product of the sulphation process, and even nitrate, nitrite, chloride, fluoride and oxalate ions in exposed specimens. In the first exposure months the concentration of pollutants deposited was very high while subsequently it lessened, probably because of wind and/or rain removal. Moreover, unsheltered samples underwent the highest washing-out, confirmed by the lowest anions concentrations and the contemporarily surface erosion.

Recently, samples of typical Florentine lithotypes (Carrara marble, Pietraforte, Pietra Serena) were exposed for 24 months outdoor in an historic building in the centre of Florence, in partially sheltered condition and located vertically, horizontally and inclined, in order to assess the effect of soluble and carbon fractions of particulate matter. The preliminary results of analyses (Fibre Optic Reflectance Spectroscopy_FORs, Spectrophotometry, Total reflectance-Fourier Transform Infrared Spectroscopy_TR FT-IR, SEM-EDX, IC, carbon speciation with CHNSO analyser and environmental monitoring campaigns) were presented in Bonazza et al., 2013. Overall, horizontally exposed samples experienced the highest effects induced by pollution impact: variation in total colour (and in details towards blackening and yellowing), presence of ions (mainly sulphate, nitrate and chloride) and changes in the FT-IR spectra probably due to the deposition of combustion products (principally organic carbon fraction). Considering the different lithotypes, Carrara marble was more vulnerable to pollution impact in respect to the other two stones.

Further exposure tests were performed by Comite et al. (2017) by horizontally exposing samples of marble (Carrara Marble) and limestones (Noto and Comiso stones) in two Sicilian cities, Palermo and Catania, for 2 years, in sheltered and unsheltered conditions. As expected, sheltered samples underwent the highest deposition of particulate matter and darkening and yellowing effects. These affected mainly Noto stone characterised by higher porosity and surface roughness than the other studied lithotypes, highlighting as the

stone features influence the change of total colour. Moreover, vehicular traffic as well as soil dust seemed to be the main sources of PM deposition.

Additionally, atmospheric monitoring campaigns performed outdoor close to historic monuments provide further information about those gases and particles potentially dangerous for the conservation of the cultural heritage but they are still scarce. In this context, Nava et al. (2010) and Ghedini et al. (2011) analysed soluble and carbon fractions of particulate matter monitored in proximity of Palazzo Vecchio and Baptistery in Florence, respectively. Recently, the Italian Institute for Environmental Protection and Research (ISPRA) and the National Institute for Conservation and Restoration (ISCR) of Italy studied the blackening of stone samples, along with copper and glass specimens, exposed close to air quality monitoring stations in Rome for 3 years (2013-2016) in order to compare colour variation with the amount of PM10 monitored over time (Gaddi et al., 2017). Auras et al. (2018) assessed the atmospheric concentrations of NO₂ and HNO₃ beside soiling and anionic concentration of deposit on Carrara Marble samples horizontally placed outdoor for one year in German cities. Despite high amount of NO₂, the deposition of NO₃⁻ on stone specimens resulted to be limited. Particulate matter was also characterised both on stone samples and quartz fibre filters passively exposed on the façade of Milan cathedral (Fermo et al., 2018) and in a more congested site of Milan (Ferrero et al., 2018). However, lacks still remains in determining the real deposition of particulate matter per surface unit, mostly concerning the carbon fractions.

1.3. DAMAGE FUNCTIONS

The amount of damage induced to building materials by environmental parameters can be described by damage functions. These are mathematical functions able to connect the degradation of cultural heritage to different variables changing over time, such as chemical attack, heating and cooling cycles, and freeze-thaw cycles for stone and masonry materials, metals, glass, and wood. In particular, the extent of damage that will result from a given amount of pollutants is known as dose-response function. A *dose* of a pollutant depends on both the concentration and the time of exposure and therefore represents the quantity of pollutant actually deposited on a surface, while *response* is recorded either as the amount of material mass loss or loss in thickness per annum or as variation in surface soiling. Nevertheless, the dose is often replaced by the concentration and thus implicitly hypothesising a direct relation between the concentration and the deposition of the pollutant. In this case, dose-response function assumes a broader sense and it is also utilised the term “exposure-response function” (Watt et al., 2009). All these equations assume an added value when they are combined with acceptability criteria, for example in the context of risk management, providing a good basis for the development of standards and the administration of time for cleaning and conservation/replacement procedures.

The early dose-response functions concerned the corrosion of materials of cultural heritage. One of the first methodical field exposure programme able to simultaneously measure corrosion attack of steel and zinc and SO₂ concentration was carried out by Gerhard Schikorr and Ina Schikorr during the period 1939 to 1942 in Berlin, Germany (Watt et al., 2009). They quantified the zinc corrosion attack in µm per year (R_{Zn}) as directly proportional to the concentration of SO₂ (µg m⁻³) multiplied by a value equivalent to 0,044:

$$R_{Zn} = 0,044[SO_2] \quad (1)$$

This equation resulted very similar to a series of functions that were developed in the following 30–40 years, all of them involving SO₂ as the main explanatory factor and with the likely addition of other parameters such as acidity, wetness and temperature terms.

Returning to the topic at hand (i.e. stone), literature reports different functions relating to the surface recession of stone. Concerning the dose-response equation resulted from the elaboration of data collected during the ICP-Materials and MULTI-ASSESS Projects (see § 1.2), two sets of functions have been developed for limestone (Watt et al., 2009): one for the SO₂ dominating situation, based on data from the original exposure (1987–1995), and the other for the multi-pollutant situation, on the basis of data recorded during the period 1997–2001 concerning SO₂, HNO₃ and PM₁₀. These functions have demonstrated to be useful for mapping areas of increased risk of corrosion and calculating the corrosion cost. Furthermore, a more detailed overview of dose-response functions about surface recession of stone is provided by Bonazza et al. (2009). Among these, the Lipfert function (Lipfert, 1989), which takes into consideration karst effect, acid precipitation and dry deposition of SO₂ and HNO₃, was used for mapping the surface recession of carbonate stones within the EU FP6 NOAH’s ARK Project (Sabbioni et al., 2012). It is noteworthy the comparison of three different functions (the Lipfert, ICP and MULTI-ASSESS ones) performed by Grossi et al. (2008) in order to predict the recession rate of calcareous stones for Oviedo, Paris and Prague from estimates of climate and air quality. Generally, these functions disagree quantitatively because of their different controlling parameter based on precipitation, SO₂, multi-pollutants or humidity. Nevertheless, their results were fairly concordant in the last decades of the twentieth century while higher differences were calculated for the future, when damage functions have to work under low pollution conditions.

Another damage to building materials that has to be measured and monitored for a better risk management is soiling. Beloin and Haynie (1975) first proposed the idea that soiling could be quantified by comparing the reflectance of a soiled surface with that of the bare material. They exposed six building materials (painted cedar siding, concrete block, brick, limestone, asphalt shingles and window glass) for two years, at five different sites in USA in exposed condition (Figure 1.7). In addition to reflectance variation, total suspended particles (TSP) and environmental parameter were measured during the exposure period. The results showed that soiling of paints was directly proportional to the square root of dose, the latter defined as the product of particulate matter concentration and exposure time:

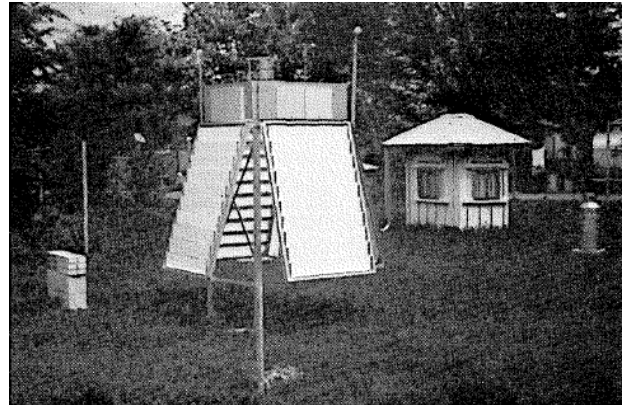


Figure 1.7 Arrangement of materials at each site (Beloin and Haynie 1975).

$$R = R_0 - k \sqrt{PMt} \quad (2)$$

where R = reflectance after time t ; t = time; R_0 = initial value of reflectance; k = constant; PM = particulate matter concentration ($\mu\text{g m}^{-3}$). However, poor correlations were obtained for concrete, limestone and window glass. Other American researches noticed that coarse particles initially contribute more to soiling of both horizontal and vertical white surfaces (SEM stubs and wooden boards) than fine mode particles but the first ones are easily removed by rain (Haynie and Lemmons, 1990; Creighton et al., 1990). Anyway horizontal surfaces are soiled faster than vertical surfaces. A more detailed overview of the results of field studies is described in Watt and Hemilton (2003).

In addition to the initial field studies, which produced empirical relationships between soiling rate and air pollution, theoretical model of soiling was required. At the end of the 1980s, the researches carried out by Haynie and Lanting, respectively, laid the foundation for the development of an exponential model to describe soiling rate (Watt et al., 2008 and relative references). Haynie assumed that soiling is equal to the contrast in reflectance of the bare substrate not covered by particles ($R_0(1-X)$) plus the reflectance from the particles (R_pX), where X is the fraction of surface covered by particles (Brimblecombe and Grossi, 2004). Therefore, if particles have a diameter bigger than the wavelength of the light:

$$R = R_0(1 - X) + R_pX \quad (3)$$

He also stated that under constant conditions, the loss in reflectance of surface was directly proportional to the surface area of the material covered by deposited particulate matter. In particular, all particulates deposited from the atmosphere would contribute to soiling and the differences in contribution seemed to be proportional to particle size and deposition velocity, not composition and related optical properties. Thus, after integration:

$$X = 1 - \exp(-kt) \quad (4)$$

where k is a function of particle distribution and dynamics and t is time. As a result of substitution the reflectance after a certain time is equivalent to:

$$R = R_0 - (R_0 - R_p) \cdot [1 - \exp(-kt)] \quad (5)$$

or

$$R = R_p + (R_0 - R_p) \cdot \exp(-kt) \quad (6)$$

On the contrary, Lanting declared that the exposed area was covered at a uniform rate and that the loss in reflectance is proportional to the thickness of the deposited film. However, while Lanting considered that only particulate elemental carbon contributed to blackening, Haynie assumed that all particulates deposited from the atmosphere would provide a reflectance change. The theoretical basis of both models were explained by Mansfield and Hemilton (1989) and Watt and Hemilton (2003). In the case the reflectance of deposited particles (R_p) is much lower the initial reflectance (R_0), i.e. $R_p=0$ (total blackness), many authors reduced the equation 6 to the following equation, which is considered as the basic exponential relationship and frequently used in the soiling studies:

$$R = R_0 \cdot \exp(-kt) \quad (7)$$

where R = reflectance after time t , t = time, k = constant.

Therefore, the mathematical theories for the growth of particulate matter on the material surface experiencing soiling consider that the soiling constant k is directly proportional to the amount of deposited particulate matter thus to the atmospheric concentration C , if the resuspension/removal rate Y is irrelevant:

$$k = \lambda c \quad (8)$$

Consequently, substituting into the basic exponential relationship produces the generic dose-response function:

$$R = R_0 \cdot \exp(-\lambda Ct) \quad (9)$$

where λ is the dose-response constant. Nevertheless, research studies on soiling of Portland limestone performed firstly in the United Kingdom and then extended also in Portugal highlighted that the initial stage of soiling (120-180 days) could be well represented by an exponential relationship but later the square root rate equation would fit much better the experimental results (Pio et al., 1998; Watt and Hemilton, 2003).

The exponential relationship suffers from boundary problems forcing the final reflectance of the soiled material to zero (Brimblecombe and Grossi, 2004). Thus the exponential equation can be rewritten more realistically as:

$$R = (R_0 - R_\infty) \cdot \exp(-kt) + R_\infty \quad (10)$$

where R_∞ is the reflectance after infinite soiling (which is not as close to zero as often assumed for R_p) and the reciprocal $1/k$ could be considered as a kind of “folding” time for the soiling process. However, there are still some restrictions that could lead this equation not to perfectly fit for the real process. For example, if particles are not randomly distributed soiling would proceed more rapidly and following a linear relationship that would be interrupted as the surface became close packed. Alternatively, particles could cluster together and thus the soiling could be slower than the predicted with the exponential model. In order to shed light on the choice of equations, Brimblecombe and Grossi (2004), within the CARMEL Project, compared and re-analysed earlier soiling data focussing on linear, exponential, power and square-root equations. As expected, all models work quite well for short records. Within the period of time of these experiments, properly bounded exponential model proved to be appropriate as it describes data sets where real soiling was fast or the exposure period lengthy (i.e. porous material horizontally exposed). However, some discrepancy exists

for short exposure period or where the soiling process was very low, such as in the case of materials vertically exposed. Consequently, the popularity of square-root models should be explained as many experiments finished near the point where r^2 for the square-root fit is at a maximum, just before the beginning of decreasing trend.

Considering the exponential model, R_∞ represents the final blackening of the material and depends on the areas covered by soiling particles and the original material colour. The value k (time constant), in turn, indicates the rate of soiling and likely depends on the concentration and deposition velocity of the atmospheric particles and removal processes. Therefore, k could be expressed as flux of particles to the surface. Concluding, k and R_∞ could be influenced by the amount of pollution, the orientation of the surfaces, the resuspension and the type of material (Brimblecombe and Grossi, 2004).

First results of the MULTI-ASSESS Project considered the soiling constant k to be directly proportional to the amount of deposited particulate matter and therefore to atmospheric concentration of PM_{10} (Kucera et al., 2005):

$$R = R_0 \cdot \exp(-kPM_{10}t) \quad (11)$$

where PM_{10} is expressed in $\mu\text{g m}^{-3}$.

Under the same EC project, Watt et al. (2008) exposed a set of materials, including Portland limestone, at locations in London, Athens and Krakow for 12 months in order to test the theoretical relationship between soiling and PM concentration against experimental data. For this reason, PM_{10} concentration was recorded and reflectance measured at monthly intervals over the exposure period on the surface of vertical surfaces, located sheltered from rain but prone to air movements. Applying appropriate fit to the exponential equation on the basis of the collected data, it was possible to proposed corrected dose-response functions for painted steel, white plastic and polycarbonate membrane. However, the results for limestone showed too much scatter between the plot of k by mathematical fit and PM_{10} concentration measured at each site for a prediction to be made. In addition to the chromatic heterogeneity of the stone support, the roughness of the surface seemed to interact with the deposition pattern and thus likely to lead to larger variations in deposition and accumulation than would be found in the case of a smooth surface.

Brimblecombe and Grossi (2004 and 2009) assumed in their models that the final reflectance that would be shown by the material (R_p) is more similar to the reflectance of an old black crust than to complete blackness. R_p is indeed determined as the area covered by soiling, which is considered as a balance between process of deposition and removal or resuspension. Thus the authors considered R_p related to the reflectance of the different soiling particles and the initial reflectance of the surface.

Brimblecombe and Grossi (2009) developed a new empirical model based on the flux of the elemental carbon (EC) to the surface. The accumulated flux of EC (S , unit g m^{-2}) was evaluated as:

$$S = F_{EC}t = V_{dEC}ECt \quad (12)$$

where F_{EC} is the flux of EC to the surface, V_{dEC} the deposition velocity and EC is the concentration of atmospheric elemental carbon. Therefore, the reflectance of a surface after a time t is:

$$R = (R_0 - R_p) \cdot \exp(-S/\tau) \quad (13)$$

where τ is the folding density (i.e. the surface concentration of EC required to reduce the reflectivity by a factor e), estimated as $7,2 \text{ g m}^{-2}$ in London crusts (Brimblecombe and Grossi, 2009). Considered that the blackening constant (i.e. λ , the dose-response constant of the equation 9) could be expressed as $V_{dEC}EC/\tau$, the initial rate of reflectance change of a clean stone could be written as:

$$-\frac{dR}{dt} = (R_0 - R_p) \cdot V_{dEC} EC / \tau \quad (14)$$

while the final reflectance of the crust as the reflectance of the depositing particles. Within the CAMEL Project, Brimblecome and Grossi (2008) correlated blackening data of different light-coloured stones with the atmospheric concentration of EC. The analyses showed that R_∞ varied from 75-80% in remote areas (where $EC < 1 \mu\text{g m}^{-3}$), 60-70% at urban background sites ($EC \approx 2-3 \mu\text{g m}^{-3}$) till to 30-40% in highly trafficked areas and road tunnels ($EC > 10 \mu\text{g m}^{-3}$).

As reported in Grossi (2016), previous studies assumed that the first order blackening constant is equal to $0,013 \text{ a}^{-1}$ for each $\mu\text{g m}^{-3}$ of EC or $0,0016 \text{ a}^{-1}$ for each $\mu\text{g m}^{-3}$ of PM_{10} , knowing V_{dEC} and taking 12% of PM_{10} to be as EC.

However, the aforementioned equations consider absolute rather than relative changes in reflectance. On the contrary for relative changes in reflectance, the blackening process should be written as:

$$\frac{R_t}{R_0} = \left(\frac{R_0}{R_0} - \frac{R_p}{R_0} \right) \exp(-kt) + \frac{R_p}{R_0} \quad (15)$$

Where the effect of the original surface is removed or reduced (Grossi, 2016).

Recently the use of tristimulus measurement according to the CIEL*a*b* system can give further information in addition to reflectance that highlights the presence of underway processes with different time constants. L^* is the variable lightness that changes from 0 (black) to 100 (white) while a^* and b^* represent the chromatic coordinates: $+a^*$ is red, $-a^*$ is green, $+b^*$ is yellow and $-b^*$ is blue. As described by Grossi (2016), the increasing emissions of organic matter, mainly derived by traffic combustion sources, leads to deposits rich in organic materials that are potentially attractive for biological activity and prone to be oxidized. As a consequence, this trend could result in a colour change of buildings facade towards warmer tones, as already observable in many historical buildings of the European cities (Grossi and Brimblecome, 2008). In this regard, earlier experimental measurements on stone display both variation in L^* and b^* parameters, the latter faster than the blackness. The increase in b^* could be likely be lost as the surface becomes covered by dark particles.

Consequently, it is becoming increasingly clear the need to acquire and assess data on the variation of the colorimetric parameters not only considering the reflectance (or lightness parameter) but in a larger scale. It is hoped that this will bring about the development of new damage and dose-response functions, able to better quantify and predict the damage of historic buildings in a changing environment.

The improvement of dose-response functions has practical implications for the management and conservation of cultural heritage. These models could indeed permit to estimate: the rate at which soiling will occur in the region of interest, the tolerable soiling before action and the tolerable time between cleaning. All these considerations need a broader evaluation that takes into consideration also the public perception of soiling, the intrinsic feature of the building (such as the debate whether the black crusts have to be totally removed or if they have an historic value), economic perspectives and air quality standards. Some studies started to address the problem of public perception and acceptability of soiling patterns on buildings by on-site questionnaires performed within the EC CAMEL Project (Grossi and Brimblecome, 2004; Watt et al., 2008). The outcomes highlighted that a 35% loss in reflectance triggers significant adverse public reaction. This value was adopted by MULTI-ASSESS Project as threshold for tolerable soiling before cleaning as well as 10-15 years were judged as a tolerable time between cleanings for cultural heritage objects (Kucera et al., 2005). These value together with the dose-response functions can be useful to estimate the maximum ambient air quality to which the building could be exposed to tolerable soiling. In this regard,

12 $\mu\text{g m}^{-3}$ was proposed as tolerable PM_{10} level for limestone for a period of 15 years between maintenance (Kucera et al., 2005).

2. CHAPTER 2 - MATERIALS AND METHODS

2.1. FIELD EXPOSURE TESTS

217 samples of Carrara Marble (CM, 163 samples) and Verona Red Marble (VRM, 54 samples) were prepared as polished tablets with dimensions of 12 x 12 x 2 cm in order to be exposed outdoor for field tests and further samples were prepared as reference materials. CM is a medium-fine grained metamorphic stone extracted in Apuan Alps (Tuscany), characterised by a white colour with some thin grey veins and patches. On the contrary, VRM, that is the commercial name of Rosso Ammonitico Veronese, is a nodular rose limestone with several red stylolitic joints and calcite veins. In particular, the selected stone represents the lower stratigraphic unit of the Rosso Ammonitico Veronese formation, extracted from Valpolicella area (Veneto) and commercially called Nembro Limestone. These lithotypes were selected for their almost totally carbonate composition and because they have been widely used as construction and decorative materials in cultural heritage since ancient time. Prior to exposure samples were polished as the smooth surface would allow better removal of the particulate matter deposited on samples during the exposure. CM has been exposed in Bologna, Ferrara and Florence in order to test the same lithotype in diverse environmental conditions, while VRM in Ferrara for comparing how two different stones react to the same environmental parameters.

Samples have been exposed outdoor, partially sheltered by direct rain, in urban areas strongly affected by pollution due to vehicular traffic. The exposure has been performed on: i) a terrace at the first floor of the National Research Council of Italy (CNR) in Bologna (via P. Gobetti 101), ii) on a roof terrace of Turchi di Bagno Palace in Ferrara (nowadays used by the University of Ferrara), oriented towards the rather busy Via Porta Mare at around 6 m high from the ground level, and iii) in a loggia of San Marco Museum overlooking via G. La Pira in the centre of Florence (Figure 2.1). Galvanized metallic racks were purposely built to host samples with three different exposure orientations: horizontal, oblique (tilted with 45° slope) and vertical, in order to test how positioning may influence particle deposition and its potential removal by wind-driven rain and to better simulate the real conditions of monuments. Specifically, samples have been exposed in a way that the material deposited on the exposed surface of a whole sample can be analysed every 6 months to detect carbon fractions and another one for soluble ions. Furthermore, two samples were designed for colorimetric analysis and other two ones, dedicated for further analyses, remained exposed for the complete period, as sketched in Figure 2.1 A-B. A roof was properly added to racks placed in Bologna and Ferrara to provide a partial protection from precipitation. The experimental tests started in June/July 2016 and they will finish after two years, even if samples exposure was designed in order to extend the study for further months. At the same time, 10 quartz fibre filters were horizontally placed close to stone samples in each site for 2 years on a cork sheet covered by PVC film and sealed with silicon gasket (Figure 2.1 C). These filters were exposed for monitoring the deposited atmospheric particulate matter (in terms of soluble and carbon fractions) on a filter every 6 months and compare how different substrate material (stone vs quartz filter) may affect particulate matter deposition.

Furthermore, PM monitoring campaigns were planned in the same locations every 6 months for monitoring the atmosphere close to samples racks and compare it with the material actually deposited on stone surface and passive filters.

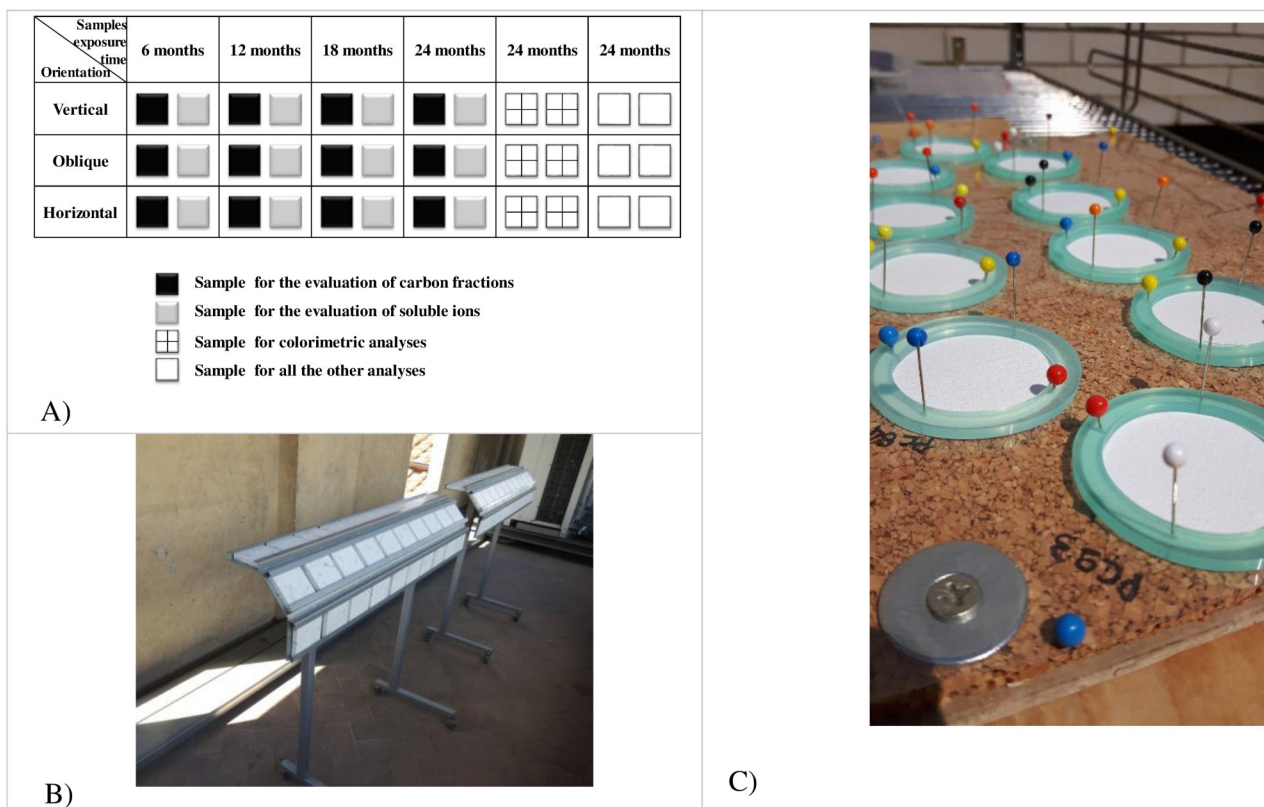


Figure 2.1 A) Model of the exposure in field of stone samples. In particular, black squares represent specimens dedicated for carbon speciation, grey ones for ion chromatography, squared ones for colorimetric analyses and white ones for further analyses. B) Racks hosting stone samples in the loggia of San Marco Museum in Florence. C) Exposure of passive filters in Bologna.

2.1.1. SITES DESCRIPTION OF FIELD EXPOSURE TEST

Sites selected as exposure locations for field study were three Italian sites: Bologna, Ferrara and Florence (Figure 2.2). The choice has been made taking into consideration different environmental conditions as well as cultural heritage wealth and use of the chosen stone materials in the architecture of the cities.



Figure 2.2 Map of sites designated for the field studies. Po Valley is highlighted in light green (<https://www.google.it/maps>).

Both Bologna and Ferrara are located in the Po Valley, a 46000 km² large area of Northern Italy extended between Western Alps and the Adriatic Sea. Po Valley is a densely populated area characterised by mild continental climate with high relative humidity throughout the year. Considered as a hot spot in Europe to air quality (Carbone et al., 2010; Perrino et al., 2014; Ricciardelli et al., 2017), this area is distinguished by a great anthropization and industrialization with relevant emissions due to industrial activities and road transport. The presence in some parts of shallow soils, extremely fertile, induced also the development of agricultural activities and livestock farming. Moreover, orographic conditions (delimited northward by the Alps and southward by the Apennines) often limits the air currents between Northern Italy and the rest of Europe. The local weak circulation and thus the air stagnation within the basin lead to longer time for the dispersion of released pollutants, promoting chemical transformation and formation of secondary compounds, especially during winter. Fog is really common during winter, which in addition to development of temperature inversion, stagnation of air masses, shallow Planetary Boundary Layer (PBL) depths (summer to winter maximum PBL height ratio ca. 2) and low wind velocity, favours the accumulation of pollutants and condensation of semi-volatile species (such as carbonaceous matter and ammonium nitrate), causing high PM episodes detected at ground level. During summer sunny days with comfortable temperatures alternate with very hot, damp days.

Bologna

Bologna (44°29'38" N, 11°20'34" E; 54 m above sea level) is the capital of Emilia-Romagna region. As its inhabitants range between 300000 and 1000000 (precisely 388000 inhabitants), it is considered a big city. First citizens of Bologna were the Etruscans followed by the Celts and the Romans. During the Middle Ages, Bologna evolved as a free municipality and it was the cradle of the oldest university in Europe (in 1088). Thanks to its past and recent musical tradition (residence for short/long periods of musicians such as Farinelli, Rossini and Donizetti) it was declared a UNESCO "city of music" in 2006 (<http://whc.unesco.org/en/list/>).

Bologna is characterised by a warm damp temperate climate with hot summer (Cfa), as shown in Figure 2.3 (Rubel et al., 2017).

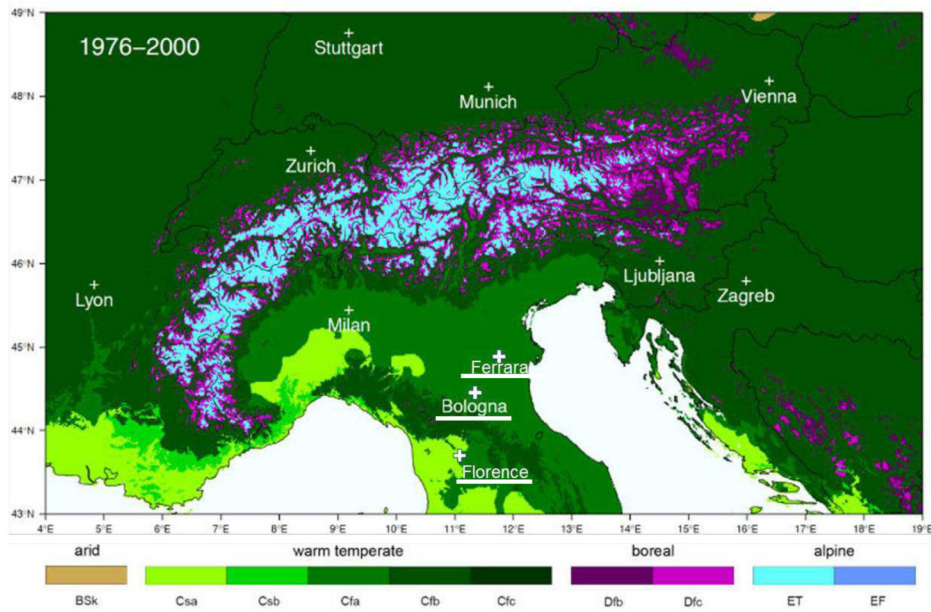


Figure 2.3 Maps of Köppen-Geiger climate classification for the greater Alpine region calculated from observed temperature and precipitation data (Rubel et al., 2017).

Average temperature ranges from about 3°C in January and 25°C in July (Figure 2.4). Mean total precipitation is of 700-800 mm, mainly concentrated during spring and autumn. From 2009 (<https://www.worldweatheronline.com>), relative humidity remained above 60% year-round with only a slight decrease during the hottest months of July and August. Wind is modest and this allows the formation of fogs and haze as well as the permanence of stagnant polluted situation.

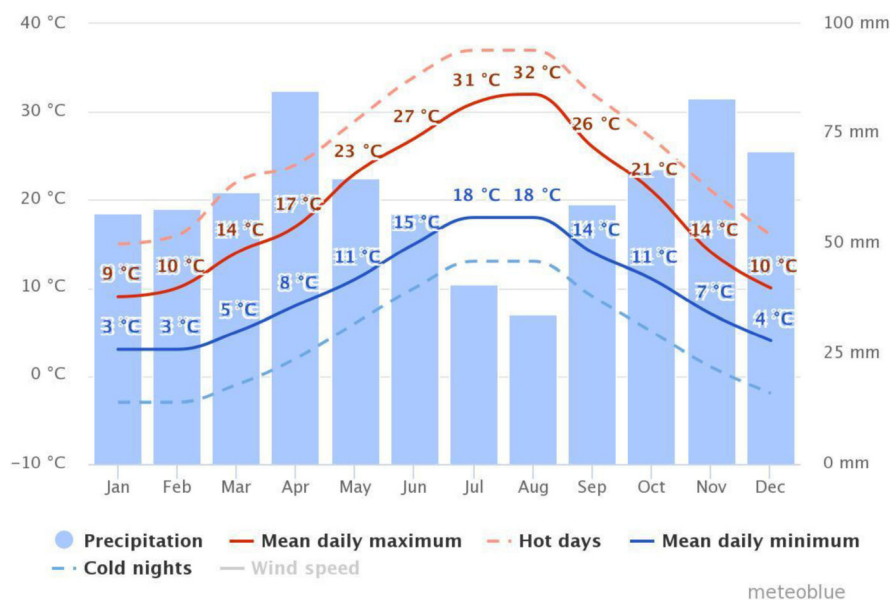


Figure 2.4 Climograph of Bologna (<http://www.meteoblue.com>).

The territory is not affected by large-scale industrial facilities but food and mechanical manufactures as well as agricultural activities are widely distributed in this site. Furthermore, a recently upgraded municipal waste incinerator is active in the city suburbs (Tositti et al., 2014). The strategic position of Bologna as crossroad between north and south of Italy and also between western and eastern sides of Po Valley cause a large-scale

transportation by railway, aviation as well as light and heavy duty traffic. It is indeed surrounded by congested orbital roads that connect the main arterial road to the biggest Italian cities.

Considering the architectural viewpoint, Bologna made primarily use of clay to realize bricks for its historic buildings due to the easy availability of this material in the surroundings (Del Monte, 2008). Moreover, pits of sandstones (soft or more cemented and thus more resistant) and selenite were spread in the area. In addition to these lithotypes, other more precious stones (such as Istria Stone and Verona Red Marble) were imported by river trade from the Romans and occasionally at later dates (for example, Verona Red Marble was used for the incomplete covering of San Petronio Basilica).

The selected site for the exposure of samples and PM monitoring is the National Research Council of Italy (CNR), located in via P. Gobetti 101 (Figure 2.5), in the Navile district.

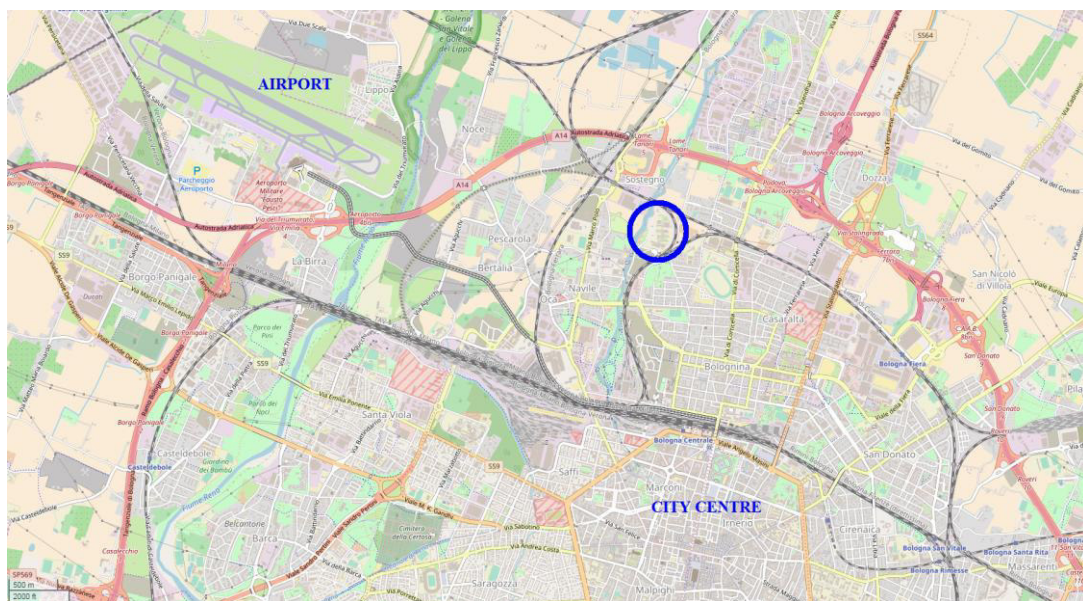


Figure 2.5 Map of Bologna. The blue circle highlights the position of the National research Council of Italy (<https://www.openstreetmap.org>).

Close to the CNR there are a rail network (as the crow flies, at 500 m there is the busy railway line Bologna-Ferrara while less than 100 m a line for cargo trains) and the congested *European Route E45* and highway *A13* (as the crow flies, at 900 m and 1700 m, respectively). It should be stressed also the presence of the international airport *Bologna Guglielmo Marconi Airport* almost 3 km far from the CNR.

In particular, rack hosting samples was placed in a terrace, at the first floor, close to the CNR Research Area Library while equipment for monitoring the PM was located on the ground close to equipment of Supersito Project with filters sampling at around 1,70 m high (Figure 2.6).

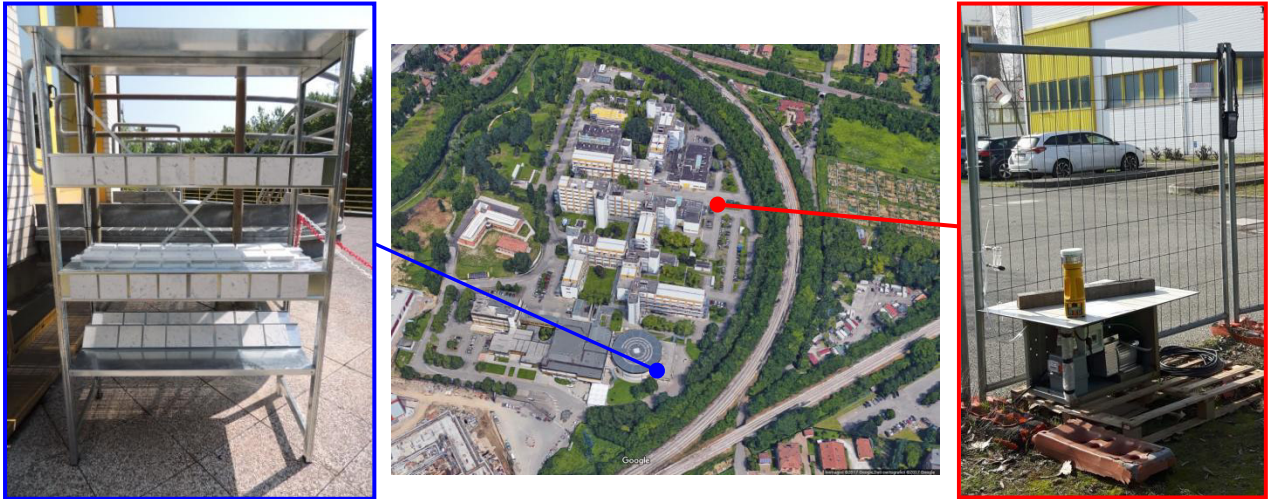


Figure 2.6 Position of rack hosting stone samples and passive filters (squared in blue) and PM as well as bioaerosol monitoring campaigns (squared in red).

Ferrara

Ferrara (44°50'7.07" N, 11°37'11.51" E; 9 m above sea level) is a city of roughly 132000 inhabitants located in Emilia-Romagna region. Ferrara is an historic city, subjected to numerous urban planning schemes from the 14th to 16th centuries, which made it the first Renaissance city to be developed by a complex urban plan. This plan harmoniously combined Middle Age and Renaissance buildings and favoured a general balance of the whole city rather than accentuate the beauty of individual buildings. It resulted in the formulation of the humanist concept of the *ideal city* and represented a criterion that has designated Ferrara as UNESCO World Heritage Site (<http://whc.unesco.org/en/list/>). Therefore its cultural preciousness should be preserved and be appreciable also by the posterity. Anyway, its position and the typical environmental conditions have led Ferrara to face humidity problems induced both by capillary rising damp and thick winter fog. The territory of Ferrara is indeed located in the Po delta and developed on river sediments (Figure 2.7). The area underwent to numerous and important reclamation works of the swampland, started firstly by the Este domain and carried on during the 20th century (<http://www.bonificaferrara.it>).



Figure 2.7 Ancient map of Ferrara area of 1568 (town archive of Ferrara, <https://upload.wikimedia.org/wikipedia/commons/d/d2/Delta-P%C3%B4-1568.jpg>).

Concerning the Köppen-Geiger climate classification, Ferrara is characterised by a warm damp temperate climate with hot summer (Cfa) (Rubel et al., 2017) (Figure 2.3). During the year the temperature ranges from 0°C to 32°C and the precipitations occur mainly as thunderstorm during summer and as light rain during the other seasons (Figure 2.8). Even if Ferrara is not so much rainy, it is characterised by high relative humidity that implies the presence of fog in autumn and winter or muggy weather during summer. The prevailing winds blow westerly and secondarily from NE and SE.

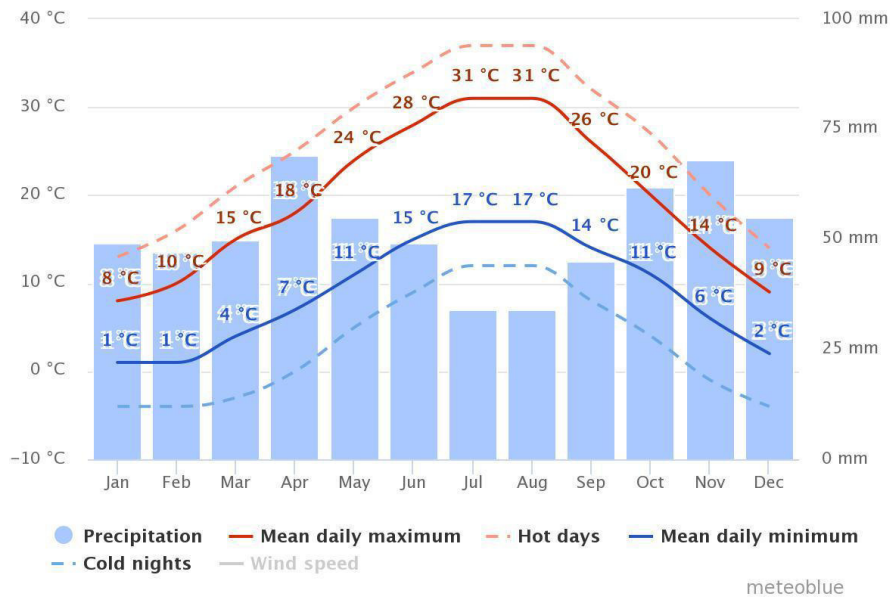


Figure 2.8 Climograph of Ferrara (www.meteoblue.com).

Even if Ferrara is an historical city and the tertiary economic sector has grown over last years, industry (mainly chemical one) as well as agricultural sector (mostly farming) are extensively developed in the city and surroundings (<http://www.fe.camcom.it/cciaa/cenni-sull-economia-provinciale>).

Taking into consideration the geology of the area, Ferrara is distinguished by the absence of quarries. This has induced the employment of clay materials for the production of brick as well as the import of stones mainly from territory close to Verona, Vicenza, Padua and Istria. Among lithotypes, Verona Red Marble, Vicenza limestone, trachyte and Istria stone were rather used in Ferrara architecture. This trade was favoured by the presence of waterway opportune for river transport and by politico-economic collaboration with governments of Vicenza and Verona, mainly during the Middle Age and Renaissance (Grillini, 2006). Stone was mainly used as architectural elements (as gate, capitals, finial of windows and sculpted cornices) for ennobling the hosting building and highlighting its importance.

The area selected for the exposure of samples and PM campaigns is located at Palazzo Turchi di Bagno (Corso Ercole I d'Este, 32), on the side of the palace oriented towards the rather busy Via Porta Mare (Figure 2.9). Palazzo Turchi di Bagno, located in front of the illustrious Palazzo dei Diamanti, is a Renaissance architectural work designed by Ar. Biagio Rossetti. From 1962 it became the seat of the botanic garden (placed backward) and from 1964 it has hosted some university branches. In a straight line, the building is 1400 m from the train station, less than 3000 m from the Petrochemical area of Ferrara and at around 4400 m from the highway A13.

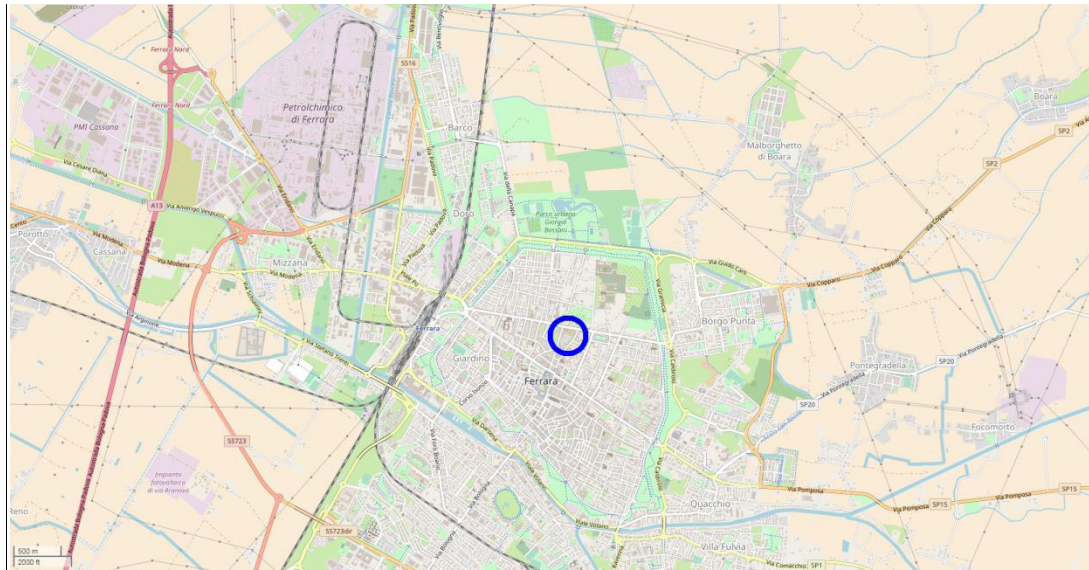


Figure 2.9 Map of Ferrara. The blue circle highlights the position of Palazzo Turchi di Bagno (<https://www.openstreetmap.org>).

Specifically, rack hosting samples and passive filters was placed on the roof terrace at the first floor of the Palace (around 6 m from the ground level) but other 9 stone samples were arranged obliquely in the same building in a window of the Museum of Palaeontology and Prehistory P. Leonardi, facing Corso Porta Mare (Figure 2.10). First PM campaign was begun on the roof terrace, close to the shelving, and then assisted by one more instrumentation at the ground floor in the Botanic Garden due to logistical problems (see Figure 2.10). Nevertheless, further campaigns took place only at the ground floor with filters sampling at around 1,80 m high from the ground.

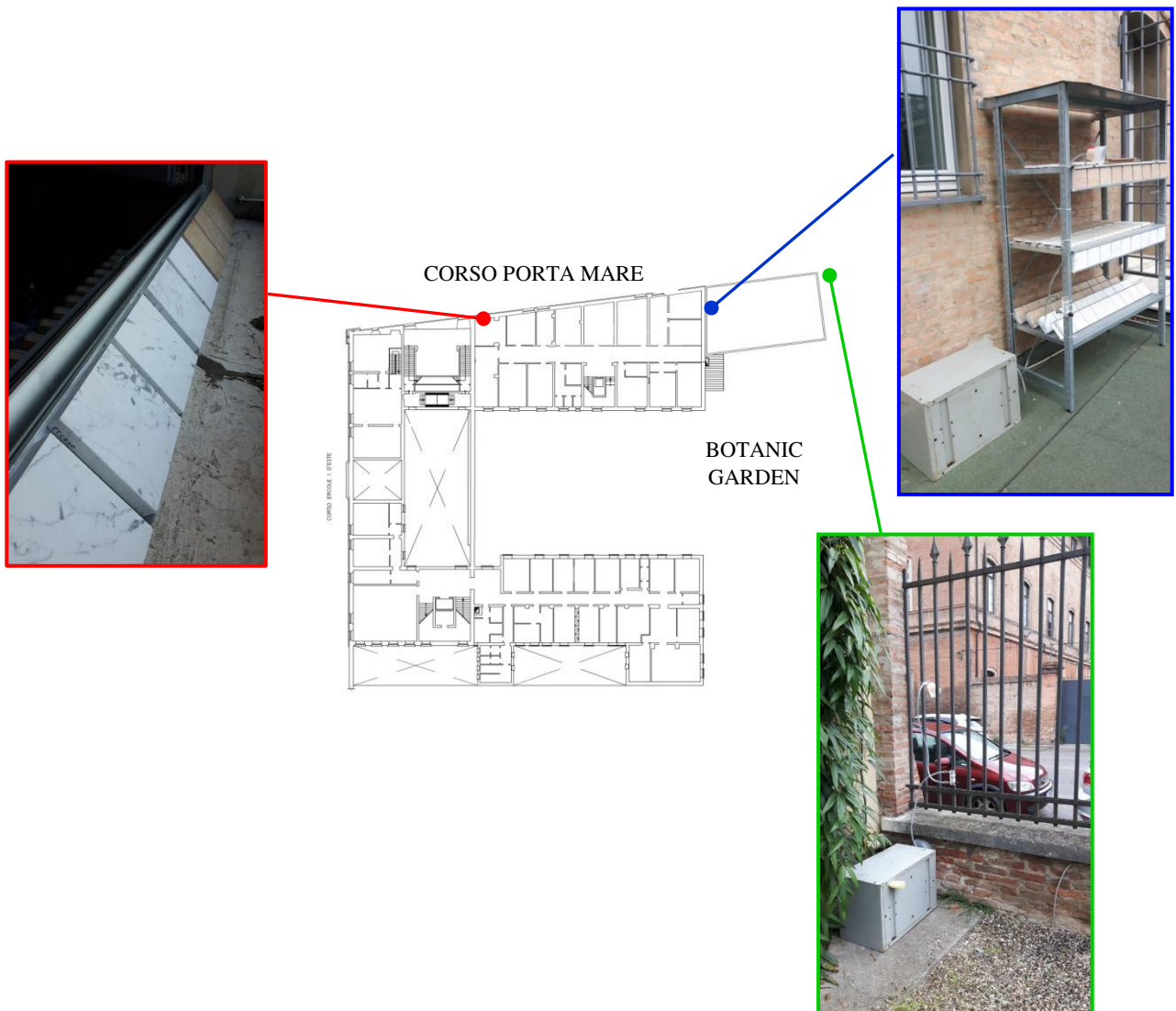
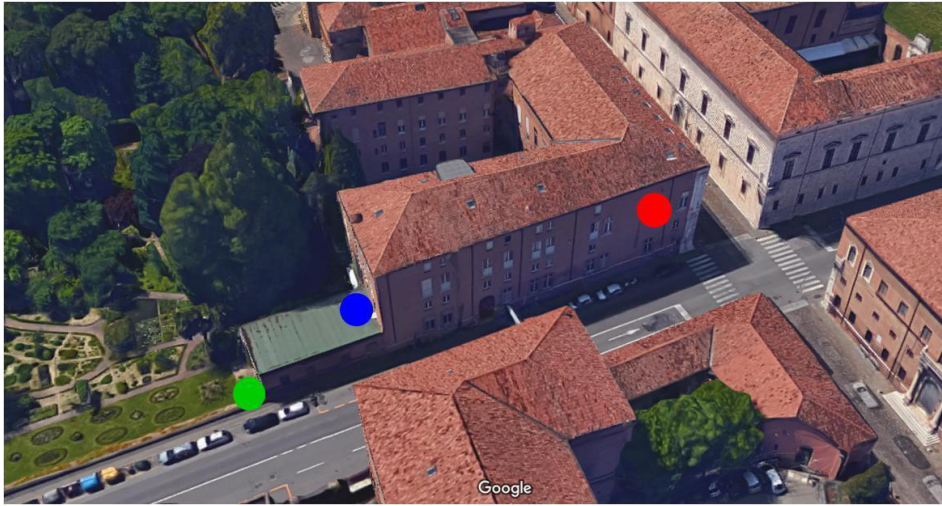


Figure 2.10 Location of rack hosting stone samples and passive filters (in blue) and further stone specimens (in red) in Ferrara. Green dot indicates the placement where PM monitoring campaigns were carried out from winter 2017.

Florence

Florence (43°47'0" N, 11°15'0" E; 50 m above sea level) is the capital city of Tuscany, a region located in the centre of Italy, and is about 80 Km east of the sea. The amount of Florentine inhabitants updated in June 2017 is of 377596 (http://statistica.fi.it/opencms/opencms/MenuPrincipale/Dati/Popolazione_Firenze). The Arno River runs east and west through the city and can represent a risk for this city of art if extreme precipitation events occur. Floods have been part of the Arno River history and have been recorded back to the 12th Century (Galloway et al., 2017). In particular, the disastrous flooding in 1966 caused 38 deaths in Florence and its province as well as damaged or destroyed millions of works of art and rare books.

Florence, built on the site of an Etruscan settlement and later ancient Roman colony of Florentia, was the birthplace of the Renaissance and reached its highest splendour during the early Medici period (between the 15th and 16th centuries), achieving noteworthy cultural and economic development. Its extraordinary artistic activity and its integrity over the years are still observable among the Medieval narrow street and imposing Renaissance buildings of the city centre. Michelangelo, Leonardo da Vinci and Botticelli as well as Dante Alighieri, Petrarch, Giovanni Boccaccio and Niccolò Machiavelli were only some of artists and poets linked to Florence. Moreover, Florence influenced the development of architecture and fine arts, first in Italy, and then abroad. Thus its city centre was included in the UNESCO World Heritage List in 1982 (<http://whc.unesco.org/en/list/>). Florence continues to attract tourists from all over the world. However, the important influxes of tourist unfortunately favour urban traffic that along with traffic induced by residents and topographical configuration of Florence (a closed basin, encircled by hills) cause recurrent heavy pollution episodes.

Florence is characterized by a mild temperature in winter, with mean temperature around 7°C, and hot summers (mean temperature around 24°C) (www.meteoblue.com). The precipitations are more pronounced in the intermediate seasons and in winter while the summer is dry (Figure 2.11). The relative humidity is substantial during the coolest months (around 70-80%) while it remains between 65-68% in spring and summer (<http://www.climatemps.com/>). During the late-afternoon of summertime winds blow from south-west to north-east while moderate to strong northern and north-eastern winds prevail during winter.

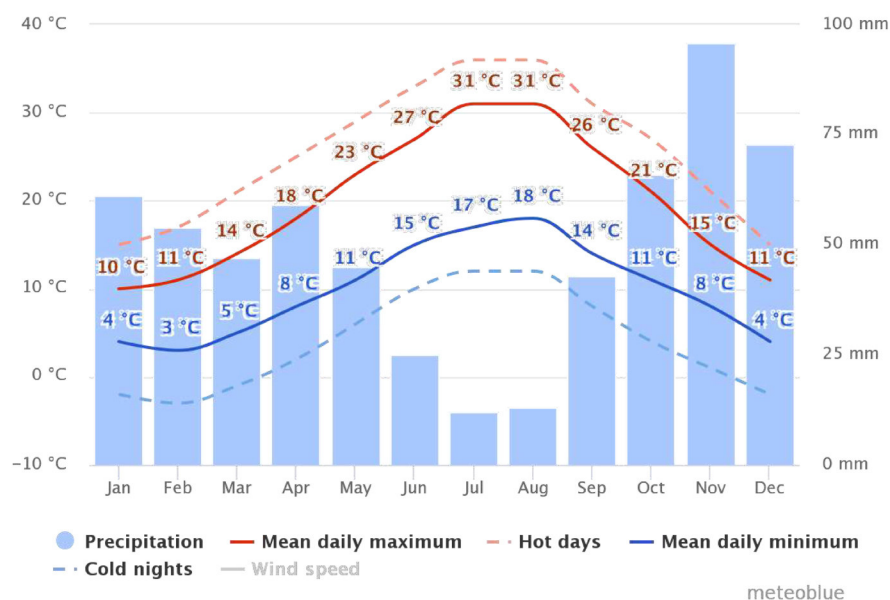


Figure 11 Climograph of Florence (www.meteoblue.com).

Considering the Köppen-Grieser's climate classification (Rubel et al., 2017), Florence belongs to the area at the border between the warm climate with hot dry summer (Csa) and the warm humid climate with hot summer (Cfa) (Figure 2.3).

Business linked to tourism supplies by far the most of the Florentine economy. However, the capital of Tuscany has an ancient experience also in leatherwork and textile industry as well as some leading sectors include mechanical engineering, fashion, pharmaceuticals, food and wine.

Observing the Renaissance architecture of Florence, most of buildings are made by local sedimentary rocks classified as Pietraforte, Pietra Serena and Pietra Bigia (Sağlar Onay and Ricci, 2013). Many of the quarries were located along the River of Arno and thus these lithotypes were easily transportable to Florence. Pietraforte is a yellowish sandstone with carbonic cement. In English it means "strong stone" because of its resistance to compression and atmospheric agents and it was therefore used as the main structural building material in the Renaissance Florence. On the contrary, Pietra Serena means "calm stone" because it is more workable respect to Pietraforte thanks to its clayey cement but it is more prone to atmospheric weathering. Its workability induced Pietra Serena to be mostly used as decorative building material (e.g. columns, cornices and arches) even if the Etruscans utilized it to build the city walls of Fiesole for overlooking Florence (Sağlar Onay and Ricci, 2013). Moreover, pavements, squares and streets were mainly built with Pietra Bigia. However, other kinds of stones were used in the Florentine architecture such as pinkish marly limestone (e.g. Rosso Ammonitico), Apuan Marbles (e.g. Carrara Marble) and serpentinite, used also in Florence Cathedral and Giotto's Bell Tower.

Site selected for samples exposure is San Marco Museum (Piazza San Marco, 3) on the side overlooking via G. La Pira, in the old town of Florence (Figure 2.12). The museum is located in the ex-monastery dedicated to St Mark, close to the homonymous church. The building, designed by architect Michelozzo, dates back to the 15th century and several frescos of Beato Angelico are observable on the walls.

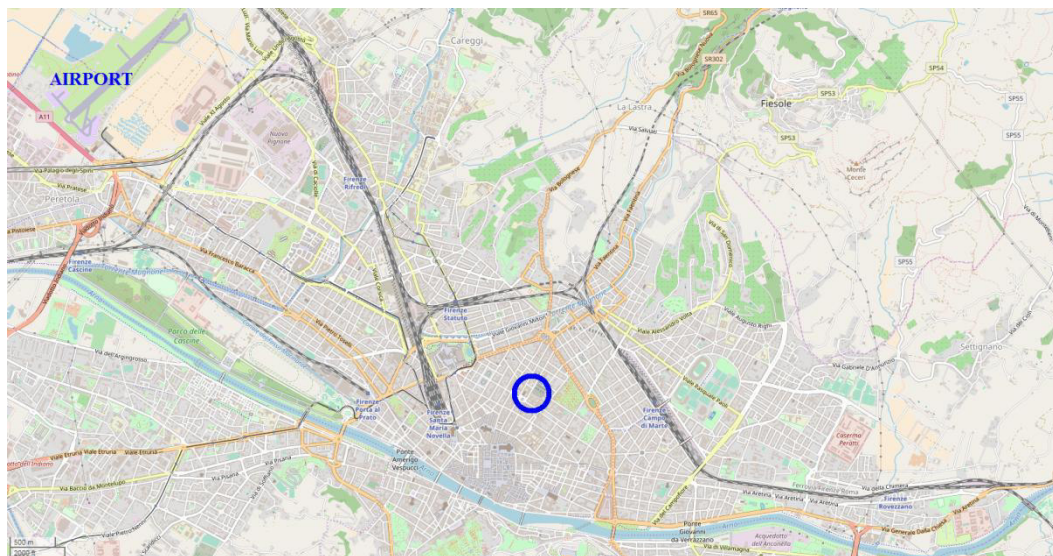


Figure 2.12 Map of Florence. The blue circle highlights the position of San Marco Museum (<https://www.openstreetmap.org>).

San Marco Museum is located close to Florence Cathedral, Santa Maria Novella train station and SS67 trunk road that bypasses the city centre (around 600 m, 1000 m and 400 m in a straight line, respectively). However, even if the Museum is positioned in a controlled traffic zone, many buses, automobiles and mopeds drive along via G. La Pira as well as Piazza San Marco represents a stop for several bus (Figure 2.13).



A)



B)



C)

Figure 2.13 Views of Piazza San Marco and the related Museum (A) and of road traffic along Via G. La Pira (B and C).

In particular, rack hosting samples and PM monitoring station were placed in a covered-roof terrace, at the first floor of the Museum, facing to Via G. La Pira (Figure 2.14).



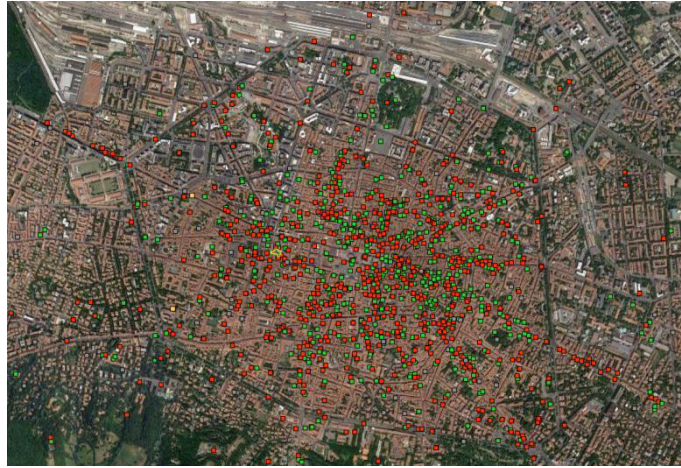
Figure 2.14 Location of racks hosting samples and PM monitoring station.

Finally, Table 2.1 summarises the main environmental and geographical features of the exposure sites selected for this research.

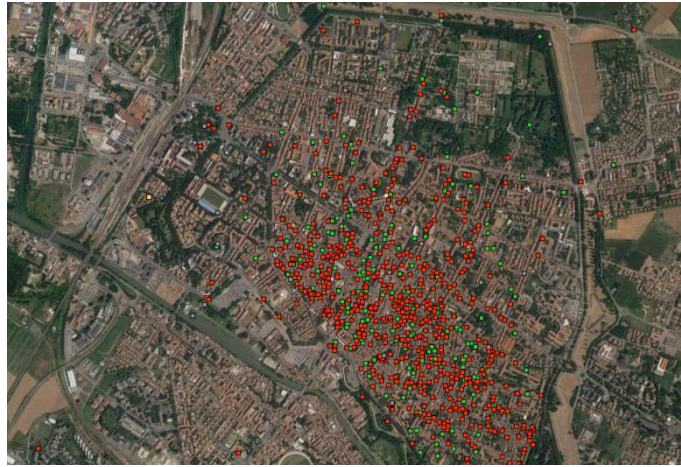
Description of sampling sites	Bologna	Ferrara	Florence
Climate (Köppen classification)	Cfa	Cfa	Csa/Cfa
Mean annual temperature (°C)	13	13	15
Warmest month (°C)	Jul	Jul-Aug	Jul-Aug
Coldest month (°C)	Jan	Jan	Jan
Annual precipitation (mm)	709	634	912
Relative Humidity (%)	74	70	70
Metres above sea level (m)	54	9	50
Total area (km ²)	141	405	102
Total population (capita) 01/01/2017 - Istat	388367	132009	382258
Population density (capita/km ²)	2754	326	3747

Table 2.1 Climate, geography and some data about population of sites selected for exposure tests (<http://www.eurometeo.com/>; <https://www.wunderground.com/>; <https://www.tuttitalia.it>)

Figure 2.15 highlights as all the selected sites are characterised by a significant amount of built heritage.



A)



B)



C)

Figure 2.15 Maps of Bologna (A), Ferrara (B) and Florence (C) at 1:14000 scale model. Red squares represent cultural heritage of stated architectural interest while green ones are those with an architectural value not yet verified (<http://vincolinretegeo.beniculturali.it>).

2.1.2. ANALYSES PERFORMED

Observation of thin sections by Polarized Light Microscopy (PLM)

Thin cross sections of stone materials were observed with polarized light microscope in order to analyse the microscopic features of marble and limestone samples before exposure. The employed petrographic microscope was an Olympus BX 51 equipped with a scanner PRIMOPLUS 32 and a vertical illuminator for reflected light.

X-Ray Powder Diffraction (XRPD)

Carrara Marble and Verona Red Marble X-ray diffraction patterns were carried out on Bruker D8 Advance diffractometer (Cu K_{α1}, α₂ radiation) equipped with a Sol-X detector in Bragg-Brentano geometry. Diffraction data were collected at room temperature (RT), in 4-60° 2θ ranges, with a counting time of 2 sec/step per 0.02 2θ step.

X-Ray fluorescence (XRF)

The concentration of major oxides (SiO₂, TiO₂, Al₂O₃, FeO, MnO, MgO, CaO, Na₂O, K₂O and P₂O₅) and trace elements (Ba, Ce, Co, Cr, Cu, Ga, Hf, La, Nb, Nd, Ni, Pb, Rb, Sc, Sr, Th, V, Y, Zn, Zr) of Carrara Marble and Verona Red Marble were quantified by a wavelength-dispersive automated ARL Advant'X spectrometer. 3 powder pellets of Carrara Marble and 6 powder pellets of Verona Red Marble (3 of sample characterised by a more greyish appearance - NBE1 - and 3 of more reddish stone sample - NBE2) were prepared grinding not exposed samples firstly by a jaw crusher and secondly by a mortar grinder with agate jar and pestle (also manual grinding with agate mortar, if necessary) and pressing the obtained powder with boric acid powder as binder. Accuracy and precision are estimated as better than 2-5 % for major elements and 10 % for trace elements (above 10 ppm).

Mercury Intrusion Porosimetry (MIP)

Porosity features were investigated on not exposed marble and limestone specimens by a porosimeter (Thermo Fisher, Pascal series 240), in order to acquire information about the porosity and pore size distribution of stone samples. Porosimetry was performed on 3 replicas of about 1x1x1 cm for Carrara Marble and on 6 for Verona Red Marble (3 on sample characterised by a greyish colour - NBE1 - and other 3 on more reddish stone sample – NBE2).

As regards the porosity range, in order to facilitate data description, interpretations refer to the porosity intervals defined according to the forces inducing fluid movement through porous media (Cardell et al., 2003), thus distinguishing between:

- microporosity, when the pore diameter is smaller than 0.1 μm and the fluid motion is caused by adsorption forces;
- mesoporosity, when the pore diameter is in the 0.1–2500 μm interval and the fluid motion is due to capillary forces;
- macroporosity, when the pore size diameter is up to 2500 μm and the fluid mobility is determined by gravitational forces.

Colorimetric Analysis

Colorimetric analysis is important for objectively quantifying the variation of samples colour measured in different time intervals compared to that before exposure. To satisfy this request, a portable spectrophotometer Konica Minolta CM-700d was employed (Figure 2.16 A).

According to the international method defined by the International Commission on Illumination in 1976 (CIELAB), colours are represented in a “colour space” and numerically expressed by three coordinates (Figure 2.16 B):

- L* (the lightness coordinate). It ranges from 0 (black) to 100 (white);
- a* (red-green coordinate), where positive data indicates redness while negative greenness;
- b* (yellow-blue coordinate), with positive values referring yellowness while negative blueness.

Colour axes are based on the fact that red-green and yellow-blue oppose each other.

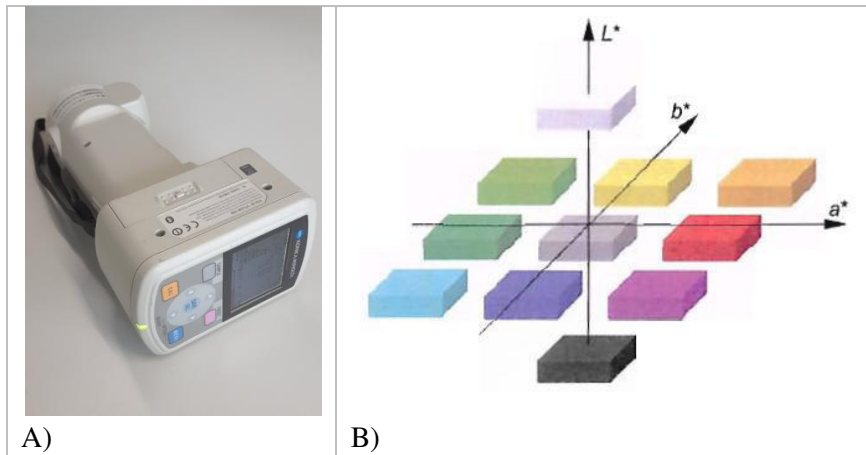


Figure 2.16 A) Portable spectrophotometer Konica Minolta CM-700d. B) CIELAB colour space (UNI EN 15886:2010).

According to UNI 15886:2010, the difference among two measurements could be described through each colorimetric parameter as:

- whitening (darkening) if $\Delta L^* > 0$ ($\Delta L^* < 0$);
- a shift towards the red (green) component if $\Delta a^* > 0$ ($\Delta a^* < 0$);
- a shift towards the yellow (blue) component if $\Delta b^* > 0$ ($\Delta b^* < 0$).

Moreover, from the combination of these parameters it is possible to calculate also the *total colour difference* ΔE^* using the following equation:

$$\Delta E^* = [(\Delta L^*)^2 + (\Delta a^*)^2 + (\Delta b^*)^2]^{\frac{1}{2}}$$

Before exposure, the measurements of the initial colour of Carrara Marble and Verona Red Marble samples were performed directly on stone surface selected to be exposed, by repeating the measure for 5 times in 5 different parts of each specimen, as shown in Figure 2.17 A. Once exposed, the surface of samples designed for colorimetric analysis were divided in 4 quarters and every six months I measured the colour on only one quarter, repeating the analysis for 5 times in 5 different points, as displayed in Figure 2.17 B. Every 6 months-period I selected a different quarter in order to avoid repeating the analysis on the same section where part of the deposited particulate matter could have been removed by the spectrophotometer during the previous analysis.

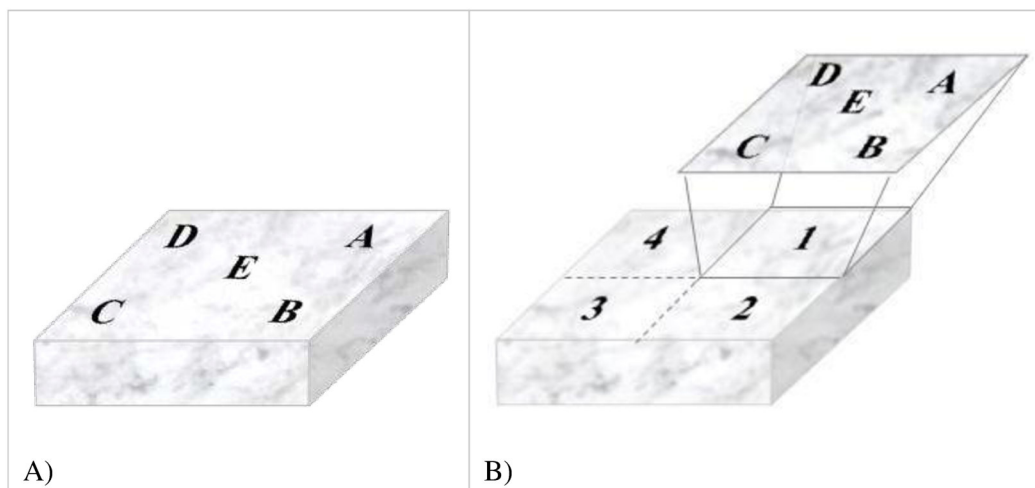


Figure 2.17 Explanation of the approach used to perform colorimetric analyses on stone samples before (A) and after exposure (B).

In particular, colorimetric analysis was carried out selecting the following features in the spectrophotometer, according to UNI 15886:2010:

- colour space: $L^*a^*b^*$;
- illuminant: D65 that represents the average daylight (including ultraviolet wavelength region) with a correlated colour temperature of 6504 K;
- observer at 10°
- measurement area: MAV 8mm
- measurement time: approximately 1 second
- light source: pulsed xenon lamp (with UV cut filter)
- Illumination system: $d:8^\circ$, which allows the illumination of the sample from all directions with a close to perfect diffuse light;
- Spectral range: 360 nm to 740 nm.

Each measure was acquired both including (SCI) and excluding (SCE) the specular component. Colour is indeed perceived when light reflects off an object and stimulates eyes' cones. The surface of an object influences the perception of object's colour because light could be reflected off in a specular or diffuse way. Specular reflection occurs more strongly on glossy surfaces, making an object appear more saturated and vivid in colour, while diffuse reflection, i.e. when light is scattered in various directions, is more evident on rough and irregular surfaces, thus object's colour appears less saturated and duller. Therefore, colour results shown in subchapter 3.1.2 refer to measure including the specular component, avoiding the influence of surface features.

Ion Chromatography (IC)

Analysis of soluble ions contribute, in combination with carbon fraction and metal content investigation, to identify the major stationary and mobile sources of air pollution that can cause the formation of damage layer on built heritage. Therefore, every 6 months from the starting of stone exposure, I collected a sample from each exposure site and for each orientation, whenever a suitable amount of particulate matter was accumulated on stone surface. The procedure for the identification of soluble ions includes firstly the separation process of soluble ions from the deposited material (extraction) and secondly the chromatographic analysis.

First of all, each sample was washed with deionised and purified water (Milli-Q by Millipore Corporation) enough to repeat the washing of the exposed stone surface several times from different orientations in order to collect the soluble ions present in the deposit. The obtained solution was then made up to a known volume and underwent extraction with ultrasonic bath for 10 minutes to obtain a homogeneous and well-dissolved solution. An aliquot of solution was filtered with pre-cleaned syringe filter (Polytetrafluoroethylene –PTFE– or hydrophilic polyethersulfone –PES– membranes) to remove particulates with a diameter higher than 0.45 μm from the sample.

For ion detection, the selected chromatography technique was the ion chromatography (IC) that separates ions based on their affinity to the ion exchanger. Water-soluble ions were analysed by an ICS-2000 Thermo Fischer Ion Chromatograph (Dionex, California, USA). Anions (Cl^- , NO_3^- , SO_4^{2-}) assessment was carried out by means of IonPac™ AS11 column utilising KOH as eluent while cations (Na^+ , NH_4^+ , K^+ , Mg^{2+} , Ca^{2+}) were detected with IonPac™ CS16 column and methylsulfonic acid (MSA) as eluent. Even if the used equipment is able to analyse also other ions (i.e. nitrite ion, formate ion, oxalate ion, acetate ion and organic ions such as dimethylammonium ion, trimethylammonium ion and methylamine ion), they were not presented here because they were always below the limit of detection and they are not the main factors of stone degradation. Moreover, oxalate ion usually undergoes degradation during the analysis and thus the detected amount (when it is above the limit of detection) may not refer to the original amount.

Results of analysis are provided in ppb but it was necessary to normalise all the investigated data to a known volume (i.e. 100 mL) to make them comparable as the volume of all analysed solutions was different. This is possible because for each sample the amount of solute remains the same while the concentration of the solution undergoes some variations by changing the solvent volume. Therefore, commensurate values were obtained through the following equation:

$$\text{Concentration}_{\text{initial}} \cdot \text{Volume}_{\text{initial}} = \text{Concentration}_{\text{final}} \cdot \text{Volume}_{\text{final}}$$

However, to obviate this problem, it is suggested for future analysis to wash all samples with a definite volume of water, for example 100 mL.

Moreover, the evaluation of the concentration of each ion per surface area is useful in the field of cultural heritage to estimate the amount and probably the contribution of each ion to stone deterioration. Since the analysed material was collected only from the flat large stone surface exposed to atmosphere (with an area of 144 cm^2), it was possible to calculate the ions soluble concentration per surface unit ($\mu\text{g cm}^{-2}$) as follows:

$$x (\mu\text{g cm}^{-2}) = [(\text{ion } (\mu\text{g}) \cdot V_{\text{solution}} (\text{mL})) / 1000 (\text{mL})] / \text{surface area } (\text{cm}^{-2})$$

Carbon Speciation and related isotopic analysis

The identification of elemental and isotopic carbon fractions (total carbon – TC, carbonate carbon – CC, elemental carbon – EC and organic carbon – OC) of material deposited on stone monuments is useful to discriminate the possible emission sources of carbon, as the deposit reflects the composition of the particulate matter to which the surface is exposed. Total carbon is indeed constituted by the following fractions:

$$\text{TC} = \text{CC} + \text{EC} + \text{OC}$$

where CC is mainly ascribable to the substrate material (i.e. carbonate stone) while OC and EC represent the non-carbonate carbon (NCC). In particular, OC derives from primary and secondary both natural and anthropogenic sources while EC is tracer for combustion processes into atmosphere. Moreover, further

information about natural and anthropogenic sources of carbon are provided by the ratio of stable carbon isotopes ^{13}C and ^{12}C ($\delta^{13}\text{C}$) expressed in per mil (‰) as:

$$\delta^{13}\text{C} = 1000 \cdot [({}^{13}\text{C}/{}^{12}\text{C}_{\text{sample}} - {}^{13}\text{C}/{}^{12}\text{C}_{\text{standard}}) / {}^{13}\text{C}/{}^{12}\text{C}_{\text{standard}}]$$

based on the international Vienna Pee Dee Belemnite (V-PDB) isotope standard. This is possible because $\delta^{13}\text{C}$ is influenced by variations in primary productivity and organic burial.

Every 6 months from the starting of stone exposure, I collected a sample from each exposure site and for each orientation, whenever a suitable amount of particulate accumulated on specimens surface, and the deposited particulate was mechanically removed with a stainless steel spatula. The methodology selected to measure carbon fractions of the material deposited on stone samples was purposely set up refining the analytical approaches tested by Natali and Bianchini (2015) and Natali et al. (2018) and involved the use of an automated elemental analyser coupled with isotope ratio mass spectrometry (EA-IRMS) and a muffle furnace. This method is based on thermally-based separation (TBS) that exploits the distinct temperature stabilities of the different carbon fractions. Specifically, three stages characterise the methodology, each performed on a different portion of the powder-like sample:

1. TC is quantified by EA-IRMS by burning the sample at 950°C;
2. OC is measured by EA-IRMS with a sample combustion at 430°C;
3. CC measure involves first the pre-treatment of the sample in a muffle furnace at 550°C for 12 h to remove all organic matter and then the burning of the residue at 950°C. The related gravimetric loss (LOI) is also determined in order to correct the elemental concentration of CC.

These phases allow to measure the amount of mentioned carbon fractions in term of weight percent and the related isotopic ratio. Finally, EC is calculated by subtracting OC and CC from TC (i.e. $\text{EC} = \text{TC} - \text{CC} - \text{OC}$) while the related isotopic ratio resulted by mass balance:

$$\delta^{13}\text{C}_{\text{EC}} = [\delta^{13}\text{C}_{\text{TC}} - (\delta^{13}\text{C}_{\text{OC}} \cdot X_{\text{OC}} + \delta^{13}\text{C}_{\text{CC}} \cdot X_{\text{CC}})] / X_{\text{EC}}$$

where X_{OC} , X_{CC} and X_{EC} represent respectively OC/TC, CC/TC and EC/TC. Additionally, EC of some samples was also determined by EA-IRMS by burning at 950°C samples previously treated by fumigation with hydrochloric acid (HCl) for around 60 h to eliminate CC and combusted at 430°C to remove OC. However, the assessment of $\delta^{13}\text{C}_{\text{EC}}$ measured by this traditional method proves to not always eliminate all the CC, depending on several causes such as kind and concentration of CC, utilised acid and operator. Therefore, results here presented refer only to values calculated by thermally based separation and mass balance as they are more reliable.

Moreover, combustion temperature of EA-IRMS for the detection of OC in deposit collected from samples exposed for 24 months was lowered to 400°C as tests performed with Elementar SoliTOC Cube, a new instrument acquired at University of Ferrara for temperature-dependent differentiation of carbon, identified this temperature as the most appropriate to measure the organic fraction. In contrast to EA-IRMS, SoliTOC Cube involves three step heating of the samples at 400°C, 600°C and 900°C and the produced CO_2 is analysed for continuous measurement of C.

The instrumentation used for measuring carbon fractions (wt%) and related isotope ratios (‰) is an Elementar Vario Micro Cube EA in line with an ISOPRIME 100 IRMS operating in continuous flow mode. Samples, in the form of powder, are first weighted and a portion of it, for each carbon fraction to detect, is then introduced in tin capsules that is wrapped and weighed. These capsules can be loaded up till 40 mg but for this analysis the weight of each portion was usually between 1,5 mg and 10,00 mg due to the low amount of total sample. Considering that these samples have a carbon content around 12-15 %, the minimum amount

of specimen needed for an exhaustive investigation of TC and its isotopic ratio is between 0.8 mg and 1 mg. Once introduced in the Vario Micro Cube autosampler, capsules are analysed by a flash combustion. Further information about the characteristics of the instrument are described in Natali et al. (2018). For most of the samples the analyses were repeated at least twice for each fraction to minimize the effect of sample inhomogeneity and give consistency to the method. The obtained results were then corrected utilising a Carrara Marble sample calibrated at the Institute of Geoscience and Georesources of the National Council of Researches of Pisa and a synthetic sulphanilamide provided by Isoprime Ltd as reference materials.

This analytical methodology intends to improve some limits commonly found in the traditional methods used to study the carbon fractions of damage layers present on stone monuments. Literature reports for example chemical-thermal method (Ghedini et al., 2006) and thermal analysis associate with ionic balance (Fermo et al., 2015) to assess carbon speciation of damage layers. However, these conventional techniques require a quite big amount of sample (1 g in Ghedini et al., 2006) not always available in the field of cultural heritage as well as chemical pre-treatments that can lead to C losses with consequences on elemental and isotopic values (see Natali et al., 2018 and related references). Furthermore, some methodologies entail a combination of different analyses, for example CHN analyses (to quantify TC and EC + CC) with ion chromatography (Cuccia et al., 2011, Fermo et al., 2015) or thermo gravimetric (TGA) and differential scanning calorimetric (DSC) analyses (La Russa et al., 2017) in order to estimate calcium carbonate content, implying more steps and the employment of different techniques. On the contrary, this thermally based carbon separation provides reliable results exploiting the change of combustion temperature in order to match the specific destabilization conditions of the targeted carbon compounds. In addition, isotope ratio mass spectrometry represents a further tool to complement the TSB method and allows the validation of the carbon pool delineation. Furthermore, this methodology is quite rapid, with limited sample manipulation and requires low amount of sample (the total quantity of each sample utilised for carbon speciation is in between 6 mg and 36 mg).

Environmental Scanning Electron Microscopy (ESEM-EDX)

Environmental Scanning Electron Microscopy and micro-chemical investigations analyses were performed to observe the morphological features of particulate matter deposited on stone samples as well as to identify its main chemical composition. For this purpose, deposited material was collected from different areas of stone sample surface remained exposed for 24 months through adhesive stubs. A ZEISS EVO LS 10 with LaB6 source was utilised in backscattered mode applying 15-20 kV acceleration voltage. As an ESEM and not a traditional SEM was selected, the analysis did not need any preparation and coating of sample surface.

Inductively Coupled Plasma Mass Spectrometry (ICP-MS)

Chemical analysis in terms of trace elements of stone substrate and material accumulated on stone samples was performed by Thermo Electron Corporation X Series spectrometer, with a collision cell (CCT^{ED}) for the reduction/exclusion of main polyatomic and isobaric interferences.

Sample preparation provided for grinding of stone substrates while powdered material accumulated on stone samples was carefully mechanically removed with a plastic spatula from the exposed surface of stone specimens remained outdoor for 24 months. At this exposure period, it was possible to collect an amount of material enough to perform ICP-MS (around 150-200 mg) only from horizontally exposed samples. In order to reach a sufficient amount of material, deposited material was collected from the surface of 6 samples in Bologna (BCH2, BCH3, BCH4, BCH5, BCH1 and BCH15 for a total weight of 158.56 mg), 2 Carrara Marble (PTCH19 and PTCH20 for a total weight of 312.44 mg) and 3 Verona Red Marble (PTNH20, PTNH23 and PTNH5 for a total weight of 281.87 mg) samples in Ferrara and 2 specimens (SMCH11 and SMCH13 for a total weight of 319.50 mg) in Florence. The quantity of material collected from Ferrara and Florence samples allowed to duplicate the analysis.

About 150 mg of each samples were put in a Teflon digestion vessel for the digestion process. First 3 mL of HNO₃ (65% in distilled water, Suprapur, Merck KGaA, Darmstadt, Germany) and 6 mL of HF (40% in distilled water, Suprapur, Merck KGaA, Darmstadt, Germany) were added in vessels with samples and heated on a hotplate at 180–190 °C until incipient drying. Afterwards, 6 mL of HCl and 2 mL of HNO₃ were added and fumigated and the resulted sub-sample underwent further reaction with 3 mL of NHO₃, 3 mL of HF and 2 mL of H₂O₂. After incipient drying, the residue was resuspended in 4 mL of HNO₃ and heated. The obtained residue was finally resuspended in 2 mL of HNO₃ and diluted to 100 mL with highly purified Milli-Q water. An internal element standard composed of Rh, Re and In was added to each solution to obtain a final concentration of 10 ppb.

The description of the analytical techniques used to assess water-soluble and carbon fractions of passive quartz filters are described in subchapter 2.2.1 as it is the same material utilised in PM monitoring campaigns.

2.2. PARTICULATE MATTER MONITORING CAMPAIGNS

The study of the microenvironment that surrounds the areas selected to expose the stone samples allows to better understand which atmospheric components can likely induce deterioration processes on stone monuments. Particulate matter (PM) monitoring campaigns were performed in Bologna, Ferrara and Florence, at the same sites selected for the exposure of stone samples and passive quartz fibre filters (see subchapter 2.1). Sampling campaigns were planned for about a week every six months in 2017 and 2018 in order to have the representativeness of the extreme seasons, i.e. summer and winter, because they are characterised by different emission sources and influenced by the height of the planetary boundary layer (PBL), i.e. the region of troposphere where atmospheric pollutants are dispersed. PBL height, directly proportional to the solar irradiance, is thus lower during winter and higher in the warm season due to thermal expansion of atmospheric gases and trend of the turbulence (Tositti et al., 2014). Moreover, further emission sources during winter, such as heating system, along with frequent thermal inversions can lead to higher concentration of particulate matter and emitted gases. Finally, also meteorological conditions (i.e. rainfall, temperature, wind speed and direction, relative humidity and cloudiness) can influence the amount and type of atmospheric components.

Atmospheric particles were collected for an exhaustive speciation including carbon fractions, soluble ions and total weight on the same filter. Since particles of all class sizes present into atmosphere can contribute to the deterioration of historic monuments, monitoring campaigns were performed on total suspended particulate (TSP) without any device for granulometric selection. The sampling was performed utilising electrical air pump, volumetric meter for air, flowmeter (working at a flow-rate of 40 L min⁻¹) and filter holder, all connected with pipes (Figure 2.18). Quartz fibre filters with diameter of 47 mm were selected in order to allow the analyses also of carbon fraction, not possible on cellulose filters. The sampling was generally planned to operate for 60 min alternated with 30 min of rest during weekdays and vice versa during the weekend, starting in the morning (around 10 a.m.) and finished at the same time of the following day. Therefore, the collected particulate matter is representative of about 16 h for weekday and about 8 for the weekend. However, some logistic problems reduced the sampling time of some days (e.g. Fridays of 2018 sampling campaigns in Bologna) but the calculation of the resulted soluble ions and carbon fractions per the collected volume makes all data comparable. Data are here presented considering sites, seasons and weekdays (Su-Sunday, Mo-Monday, Tu-Tuesday, We-Wednesday, Th-Thursday, Fr-Friday, Sa-Saturday, Wknd-weekend) in order to find analogies and differences.

The first sampling campaign was performed between 9 February 2017 and 8 March 2017 (Table 2.2). For this monitoring campaign, we were allowed to enter the San Marco Museum in Florence and the CNR in Bologna also during Saturday and Sunday and thus we changed daily the sampling filter. On the contrary, logistic problems forced us to find another place for the sampling device of Ferrara, moving it from the roof terrace close to the shelving to the ground floor in the Botanic Garden. The latter remained the sampling site of all the following monitoring campaigns.



Figure 2.18 Device utilised for PM monitoring campaign.

		Day	Start date	End date	ΔV (m ³)	Flow-rate (L min ⁻¹)	Sampling time (min)
BOLOGNA	BF11	Thursday	09/02/2017	10/02/2017	54.436	40	on 60 - off 30
	BF12	Friday	10/02/2017	11/02/2017	52.811	40	on 60 - off 30
	BF13	Saturday	11/02/2017	12/02/2017	52.274	40	on 60 - off 30
	BF14	Sunday	12/02/2017	13/02/2017	52.202	40	on 60 - off 30
	BF15	Monday	13/02/2017	14/02/2017	51.615	40	on 60 - off 30
	BF16	Tuesday	14/02/2017	15/02/2017	52.092	40	on 60 - off 30
	BF17	Wednesday	15/02/2017	16/02/2017	43.747	40	on 60 - off 30
FLORENCE	SMF11	Thursday	16/02/2017	17/02/2017	52.736	40	on 60 - off 30
	SMF12	Friday	17/02/2017	18/02/2017	53.048	40	on 60 - off 30
	SMF13	Saturday	18/02/2017	19/02/2017	52.734	40	on 60 - off 30
	SMF14	Sunday	19/02/2017	20/02/2017	52.946	40	on 60 - off 30
	SMF15	Monday	20/02/2017	21/02/2017	53.070	40	on 60 - off 30
FERRARA	PTF11	Wednesday	22/02/2017	23/02/2017	58.247	40	on 60 - off 30
	PTF12	Thursday	23/02/2017	24/02/2017	60.322	40	on 60 - off 30
	PTF13	Friday	24/02/2017	25/02/2017	64.508	40	on 60 - off 30
	PTF14	Monday	27/02/2017	28/02/2017	65.429	40	on 60 - off 30
	PTF15	Tuesday	28/02/2017	01/03/2017	57.661	40	on 60 - off 30
	PTF16 *	Friday	03/03/2017	04/03/2017	39.765	20	on 60 - off 30
	PTF17	Weekend	04/03/2017	06/03/2017	132.942	40	on 60 - off 30
	PTF18 *	Weekend	04/03/2017	06/03/2017	79.883	20	on 60 - off 30
	PTF19 *	Monday	06/03/2017	07/03/2017	51.636	40	on 60 - off 30
	PTF20 *	Tuesday	07/03/2017	08/03/2017	53.761	40	on 60 - off 30

Table 2.2 Information about PM monitoring campaign performed in Winter 2017. * means that the monitoring campaign occurred at the ground floor of Palazzo Turchi di Bagno, in the Botanic Garden.

The second PM monitoring campaign was carried out between 6 and 28 June 2017 (Table 2.3).

		Day	Start date	End date	ΔV (m ³)	flow-rate (L min ⁻¹)	sampling time (min)
FLORENCE	SMF16	Tuesday	06/06/2017	07/06/2017	52.397	40	on 60 - off 30
	SMF17	Wednesday	07/06/2017	08/06/2017	54.358	40	on 60 - off 30
	SMF18	Thursday	08/06/2017	09/06/2017	54.502	40	on 60 - off 30
	SMF19	Friday	09/06/2017	10/06/2017	54.246	40	on 60 - off 30
	SMF20	Weekend	10/06/2017	12/06/2017	59.828	40	on 30 - off 60
BOLOGNA	BF18	Tuesday	13/06/2017	14/06/2017	54.595	40	on 60 - off 30
	BF19	Wednesday	14/06/2017	15/06/2017	52.980	40	on 60 - off 30
	BF20	Thursday	15/06/2017	16/06/2017	54.995	40	on 60 - off 30
	BF_21	Friday	16/06/2017	17/06/2017	50.922	40	on 60 - off 30
	BF_22	Weekend	17/06/2017	19/06/2017	59.833	40	on 30 - off 60
FERRARA	PTF_21	Wednesday	21/06/2017	22/06/2017	53.666	40	on 60 - off 30
	PTF_22	Thursday	22/06/2017	23/06/2017	53.758	40	on 60 - off 30
	PTF_23	Friday	23/06/2017	24/06/2017	53.528	40	on 60 - off 30
	PTF_24	Weekend	24/06/2017	26/06/2017	58.725	40	on 30 - off 60
	PTF_25	Monday	26/06/2017	27/06/2017	51.297	40	on 60 - off 30
	PTF_26	Tuesday	27/06/2017	28/06/2017	53.259	40	on 60 - off 30

Table 2.3 Information about PM monitoring campaign performed in Summer 2017.

Winter PM monitoring campaign of 2018 took place between 16 January and 8 February (Table 2.4). During the PM monitoring campaign of Bologna, the monitoring was performed every 30 min for technical problems, leading to 12 h of sampling per day throughout the campaign.

		Day	Start date	End date	ΔV (m ³)	Flow-rate (L min ⁻¹)	Sampling time (min)
FERRARA	PTF27	Tuesday	16/01/2018	17/01/2018	52.100	40	on 60 - off 30
	PTF28	Wednesday	17/01/2018	18/01/2018	54.876	40	on 60 - off 30
	PTF29	Thursday	18/01/2018	19/01/2018	53.834	40	on 60 - off 30
	PTF30	Friday	19/01/2018	20/01/2018	54.360	40	on 60 - off 30
	PTF31	Weekend	20/01/2018	22/01/2018	58.492	40	on 30 - off 60
	PTF32	Monday	22/01/2018	23/01/2018	43.469	40	on 30 - off 30
BOLOGNA	BF23	Wednesday	24/01/2018	25/01/2018	41.477	40	on 30 - off 30
	BF24	Thursday	25/01/2018	26/01/2018	41.984	40	on 30 - off 30
	BF25	Friday	26/01/2018	26/01/2018	14.373	40	on 30 - off 30
	BF26	Weekend	26/01/2018	29/01/2018	77.486	40	on 30 - off 60
	BF27	Tuesday	30/01/2018	31/01/2018	41.266	40	on 30 - off 30
	BF28	Wednesday	31/01/2018	01/02/2018	43.295	40	on 30 - off 30
FLORENCE	SMF21	Friday	02/02/2018	03/02/2018	52.388	40	on 60 - off 30
	SMF22	Weekend	03/02/2018	05/02/2018	59.840	40	on 30 - off 60
	SMF23	Monday	05/02/2018	06/02/2018	54.776	40	on 60 - off 30
	SMF24	Tuesday	06/02/2018	07/02/2018	52.900	40	on 60 - off 30
	SMF25	Wednesday	07/02/2018	08/02/2018	54.958	40	on 60 - off 30

Table 2.4 Information about PM monitoring campaign performed in Winter 2018.

Last PM monitoring campaign was carried out between 7 and 29 June 2018 (Table 2.5).

		Day	Start date	End date	ΔV (m ³)	Flow-rate (L min ⁻¹)	Sampling time (min)
BOLOGNA	BF29	Thursday	07/06/2018	08/06/2018	52.140	40	on 60 - off 30
	BF30	Friday	08/06/2018	08/06/2018	19.160	40	on 60 - off 30
	BF31	Weekend	08/06/2018	11/06/2018	74.791	40	on 30 - off 60
	BF32	Monday	11/06/2018	12/06/2018	50.904	40	on 60 - off 30
	BF33	Tuesday	12/06/2018	13/06/2018	50.665	40	on 60 - off 30
	BF34	Wednesday	13/06/2018	14/06/2018	51.105	40	on 60 - off 30
FLORENCE	SMF26	Friday	15/06/2018	16/06/2018	51.722	40	on 60 - off 30
	SMF27	Weekend	16/06/2018	18/06/2018	61.073	40	on 30 - off 60
	SMF28	Monday	18/06/2018	19/06/2018	55.760	40	on 60 - off 30
	SMF29	Tuesday	19/06/2018	20/06/2018	55.578	40	on 60 - off 30
	SMF30	Wednesday	20/06/2018	21/06/2018	55.689	40	on 60 - off 30
FERRARA	PTF33	Friday	22/06/2018	23/06/2018	50.992	40	on 60 - off 30
	PTF34	Weekend	23/06/2018	25/06/2018	59.741	40	on 30 - off 60
	PTF35	Monday	25/06/2018	26/06/2018	52.049	40	on 60 - off 30
	PTF36	Tuesday	26/06/2018	27/06/2018	52.258	40	on 60 - off 30
	PTF37	Wednesday	27/06/2018	28/06/2018	52.714	40	on 60 - off 30
	PTF38	Thursday	28/06/2018	29/06/2018	52.699	40	on 60 - off 30

Table 2.5 Information about PM monitoring campaign performed in Summer 2018.

2.2.1. ANALYSES PERFORMED

Preparation of quartz fibre filters

Quartz fibre filters utilised for the analysis of atmospheric PM through monitoring campaigns and passive deposition were first washed with purified water in order to eliminate any possible soluble ion and then backed at 800°C for 1 h to remove any absorbed organic matter. Filters remained in a desiccator for a night, they were later weighted and kept at room temperature until sampling. Once collected the PM, filters were weighted again (after stabilisation in desiccator) and stored in Petri dishes carefully sealed with parafilm in the fridge until their analysis. Half of the sample was used for ion chromatography while the remaining half for carbon speciation.

Ion Chromatography (IC)

Soluble ions represent an important fraction of atmospheric particulate matter and change depending on site of sampling and on the analysed dimension of PM. Ions can be directly emitted into atmosphere from natural processes such as crustal erosion and sea spray or can derive from anthropic activities (e.g. combustion, industrial and farming emissions) through the conversion of gases to particles by radical oxidative reactions into atmosphere and subsequent acid-base neutralisation. Therefore, the investigation of soluble ion present into atmosphere can help to identify the possible emissions sources of each selected sampling site.

After PM monitoring campaigns or passive exposure, a known portion of filters was put in a vial with ultrapure water and this solution was placed in ultrasonic bath for 30 minutes in order to extract water-soluble ions. Once filtered with pre-cleaned syringe filters (hydrophilic polyethersulfone - PES-membrane), an aliquot of the solution was introduced in ion chromatographer for ions detection. Filters BF11-BF20, PTF11-PTF20 and SMF11-SMF20 as well as passive filters were analysed with an ICS-1000 Ion Chromatograph (Dionex). Anions analysis was carried out by means of a IonPac AS14A (Dionex) column using 8 mM Na₂CO₃ /1 mM NaHCO₃ as eluent at 1 mL min⁻¹ flow rate and, for the detection, a conductivity system equipped with a ASRS-ULTRA suppression mode (Dionex). Cations determination was performed by means of a CS12A (Dionex) column using 20 mM MSA as eluent at 1 mL min⁻¹ flow rate and, for the detection, a conductivity system equipped with a CSRS-ULTRA suppression mode (Dionex). All the other filters were studied by an ICS-2000 Thermo Fischer Ion Chromatograph (Dionex, California, USA). Anions assessment was carried out by means of IonPac™ AS11 column utilising KOH as eluent while cations were detected with IonPac™ CS16 column and methylsulfonic acid (MSA) as eluent. The utilised equipments are able to analyse several ions, such as nitrite, formate, oxalate, acetate, dimethylammonium, trimethylammonium and methylamine ions, but it was decided to process data only about chloride, nitrate, sulphate anions and sodium, ammonia, potassium, magnesium and calcium cations as the other ions were below limit of detection (< LOD), underwent degradation process during analysis or are not ascribable as deterioration factors for stone materials.

For filters used for PM monitoring campaigns, results of the analysis are supplied as ppb but they should be modified in µg m⁻³ in order to know the amount of each soluble ion collected from quartz fibre filter per sampling volume through the following equation:

$$\text{ion concentration } (\mu\text{g m}^{-3}) = \{[(\text{ion concentration (ppb)} / 1000) \cdot V_{\text{extraction}} (\text{mL})] \cdot \text{filter area (cm}^2) / \text{punch area (cm}^2)\} / \text{sampling volume (m}^3)$$

where filter area is the sampled area (without the surface portion covered by the O-ring that secures the filter). In order to find a possible connection among different ions, Pearson correlation was measured. A Pearson correlation (ρ) is a number between -1 and 1 useful to measure the linear correlation between two variables (x and y) through the following equation:

$$\rho_{x,y} = \text{cov}_{xy} / \sigma_x \cdot \sigma_y$$

where cov_{xy} is the covariance of x and y while σ_x and σ_y represent the standard deviation of x and y, respectively. If $-1 < \rho_{x,y} < 0$, the two variables are negatively correlated while $\rho_{x,y} = 0$ means that no linear relation exist. A positive linear correlation exists when an increase of x is related to a growth of y ($\rho_{x,y} > 0$). In particular, values between 0 and 0.3 indicate a weak positive linear relationship, between 0.3 and 0.7 a moderate relationship and between 0.7 and 1.0 a strong correlation.

Results of passive filters were converted from ppb to the amount of each ion per surface unit (µg cm⁻²) through the following equation:

$$\text{ion concentration } (\mu\text{g cm}^{-2}) = \{[(\text{ion concentration (ppb)} / 1000) \cdot V_{\text{extraction}} (\text{mL})] / \text{punch area (cm}^2)\}$$

where punch area is equal to 1 cm².

Carbon speciation

Carbon fraction is an important component of atmospheric particulate matter, representing 10-43 % and 21-78 % of the masses of PM₁₀ and PM_{2.5}, respectively (Pio et al., 2011). The carbonaceous PM is composed by an organic fraction, called organic carbon (OC), and by a refractory light-absorbing component, named

elemental carbon (EC) or soot. As already described in the Chapter 1, they have different origin: EC is directly emitted by the incomplete combustion of organic material for example from traffic, domestic heating, energy production, industrial activities using different combustion fuels while OC has both primary and secondary origin. OC could indeed be directly emitted as plant debris and biological particles or from biomass burning and fuel emissions but also from gas-to-particle transformation processes in the atmosphere. Carbonaceous PM implies important effects on climate and human health but consequences of its presence are also detectable on monuments and historic buildings (e.g. soiling and black crusts formation). Therefore, information about carbon fractions present into atmosphere can provide useful information to better know the possible responsible of stone deterioration.

Carbon speciation of filters (passive filters and those pertained to PM monitoring campaigns) was carried out using a thermo-optical transmittance (TOT) method with a Sunset Laboratory OC/EC analyser (Birch and Cary, 1996), providing elemental and organic carbon concentrations. Punches of 1.0 cm² or 1.5 cm² were cut from the filters and analysed according to the NIOSH870 protocol. To ensure the accuracy of the OC and EC analysis, the analyser was calibrated (multipoint) using a sucrose solution (2.198 g/L in water, CPAchem Ltd) as external standard, as explain in Cesari et al. (2018).

The instrumentation supplies data as mass of carbon fraction per surface unit (µg cm⁻²). However, the results for monitoring campaigns should be converted in µg m⁻³ in order to know the amount of carbon fraction collected on the surface of quartz fibre filter per sampling volume through the following equation:

$$C \text{ concentration} = [C \text{ concentration } (\mu\text{g cm}^{-2}) \cdot \text{filter area (cm}^2)] / \text{sampling volume (m}^3)$$

where filter area is the sampled area (without the surface portion covered by the O-ring that secures the filter).

Bioaerosol monitoring

At the same time as aerosol monitoring campaigns, bioaerosol was assessed and quantified in Bologna at 6 and 12 months of the study. Surface Air System, in combination with laboratory culture methods (INAIL 2010, 2011), was selected as sampling method to determine the atmospheric concentration of the potentially biodeteriogenic air-dispersed viable components. This equipment was designed for indoor measurement but it could be successfully used also in outdoor monitoring. It is considered throughout the world the reference instrument for microbiological air sampling able to capture aerosol at 100% (De Nuntiiis and Palla, 2017). SAS is a portable and manageable single-stage impactor, capable to aspirate air at constant rate for a variable period through a punctured top. Air flow is thus collected on the agar surface of a Petri dish containing culture medium, suitable for the growth of the microorganisms. The Petri dishes could then be incubated to allow the development of captured microbes for later quantification and identification. The results should be expressed as colony-forming units per volume of sampled air (CFU m⁻³).

In this work, culture media suitable for the colonisation of bacteria (Plate Count Agar-PCA, Oxoid Standard, USA) and fungi (Sabouraud Dextrose Agar with chloramphenicol - SDA, Oxoid, USA) were selected. Each sampling (20 s) was conducted in double (2 PCA and 2 SDA) and generally repeated in the morning and the afternoon utilizing a SAS Super 100 (International PBI, Milan, Italy), characterised by a flow rate of 100 litres of air per minute (Figure 2.19), and Petri dishes of 90 mm of diameter. The selected location was the same of the other aerosol monitoring campaigns (Figure 2.20 A). After sampling, plates containing the specific culture medium remained in incubators at 25°C and 22°C (for fungi and bacteria, respectively) for 5-7 days for the growth of microorganisms. The developed colonies visible to the naked eye were morphologically discriminated between bacteria (with a shining and gelatinous appearance) and fungi



Figure 2.19 Surface Air System SAS Super 100 used for bioaerosol monitoring campaigns.

(more wrinkled, velvety and dusty). Then they were counted (Figure 2.20 B), adjusted by the correction table supplied by PBI and calculated as colony-forming units per volume of sampled air (CFU m⁻³). The statistical correction is necessary because more culturable spores can impact the same point of the plate during the sampling. Furthermore, a morphological analysis was performed on fungal colonies (INAIL, 2011) and it was possible to characterise some fungi genera with the help of an optical microscope.

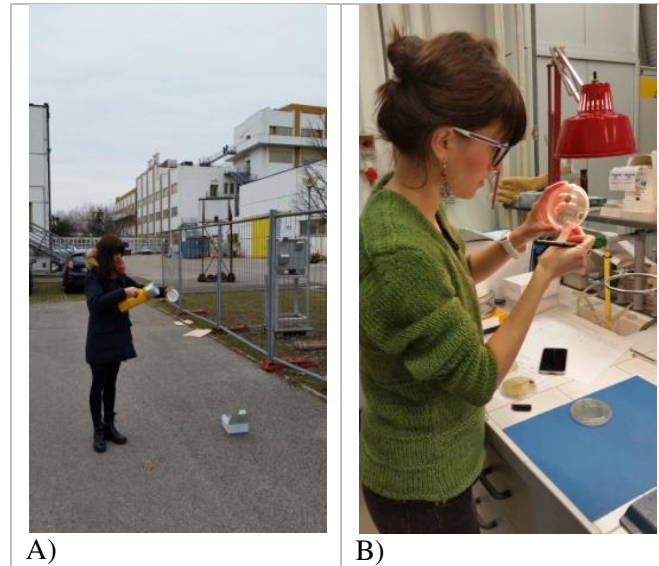


Figure 2.20 A) Sampling of viable bioaerosol with SAS at CNR, Bologna. B) Counting of the grown colonies after the incubation period.

